BAHAGIAN A – Pengesahan Kerjasama*

Adalah disahkan bahawa projek penyelidikan tesis ini telah dilaksanakan melalui kerjasama antara _____ dengan _____

Disahkan oleh:

Tandatangan : ..... Tarikh : .....

Nama : .....

Jawatan : .....
(Cop rasmi)

* *Jika penyediaan tesis/projek melibatkan kerjasama.*

BAHAGIAN B – Untuk Kegunaan Pejabat Sekolah Pengajian Siswazah

Tesis ini telah diperiksa dan diakui oleh:

Nama dan Alamat Pemeriksa Luar : .....
.....
.....

Nama dan Alamat Pemeriksa Dalam : .....
.....
.....

Nama Penyelia Lain (jika ada) : .....
.....
.....
.....

Disahkan oleh Penolong Pendaftar di SPS:

Tandatangan : ..... Tarikh : .....

Nama : .....

FAILURE ANALYSIS OF A SUBMERSIBLE PUMP SHAFT

J.KULASEGARAN S/0 JAYABALAN

A project report submitted in partial fulfilment of the
requirements for the award of the degree of
Master of Engineering (Mechanical)

Faculty of Mechanical Engineering
Universiti Teknologi Malaysia

MAY 2007

To my beloved family and friends

ACKNOWLEDGEMENT

In preparing this thesis, I was in contact with many people, researchers and academicians. They have contributed positively towards my understanding and thoughts. In particular, I wish to express my sincere appreciation and gratitude to my thesis supervisor, Professor Dr. Mohd Nasir Tamin, for encouragement, guidance, critics and friendship throughout the duration of this thesis. I am also very thankful to my supervisor's researchers especially Ms. Fethma, Mr. Hassan and Mr. Adil Khattak for their guidance, advices and motivation. Without their continued support and interest, this thesis would not have been the same as presented here.

My fellow postgraduate students should also be recognized for their support and motivation. My sincere appreciation also extends to all my colleagues and others who have provided assistance at various occasions. Their views and tips are useful indeed. I am also grateful to all my family members and especially my wife who has been always there giving her full support.

ABSTRACT

Submersible pump are widely used in a wastewater pumping station and treatment plants, to transfer sewage from a sump or wet well to other parts of the processes. Usually when a centrifugal pump is operating at its best efficiency point (BEP), the bending forces are evenly distributed around the impeller. If the pump discharge is throttled from this best efficiency point, then the fluid velocity is changed and causes the hydraulic radial imbalances load to increase at the impeller of the pump. Therefore, the shaft of the submersible pump is subjected to cyclic stresses due to this hydraulic radial imbalance loading and torsional load. This thesis mainly focuses on the distribution of stresses on the critical area of the shaft due to the imbalance loads and to determine the causes of failure to the shaft. Methodology used to carry out th e study are mainly through analytical calculation (static & fatigue) and 3D analysis (Finite element analysis & fatigue life cycle analysis). Results from both the analytical and 3D analysis shows that the pump shaft has been designed for infinite life as the fatigue life cycle is in the region of 10^{10} to 10^{12} cycles at the critical area of the shaft. Since the shaft has been designed for infinite life, the other factors such as stress corrosion cracking, pitting, cavitations and imperfection during manufacturing are suspected to be the possibilities of main contributors to the failure of the shaft, mainly due to fatigue under cyclic loading when it is in operation.

ABSTRAK

Kini, pam empar digunakan secara berleluasa di loji kumbahan najis dan di stesyen pam yang berfungsi untuk mengepam air najis dari tangki najis ke proses yang seterusnya. Apabila pam empar beroperasi pada tahap kecekapan terbaiknya, daya empar yang wujud disekitar impelernya adalah seimbang ataupun sekata. Manakala, apabila prestasi pam berganjak atau berubah daripada tahap kecekapan terbaiknya, halaju cecair yang dipam akan berubah dan menjadikan daya empar menjadi tidak sekata disekitar impeler pam empar. Jadi, ini menyebabkan shaf pam empar tersebut mengalami tegasan secara mampatan dan tegangan yang berterusan semasa beroperasi. Tesis ini merangkumi perubahan tegasan pada bahagian-bahagian kritikal shaf serta mengenalpasti punca kegagalan shaf tersebut. Oleh itu, metadologi yang digunakan untuk tesis ini adalah secara pengiraan analitikal serta analisis 3D. Walaubagaimanapun, keputusan yang diperolehi daripada kedua-dua metadologi tersebut menunjukkan bahawa shaf tersebut telah direkabentuk untuk beroperasi sehingga infiniti kitaran hidup. Secara kesimpulannya, faktor-faktor lain seperti tegasan melalui pengaratan serta kecacatan semasa pembuatan shaf tersebut adalah merupakan punca kegagalan shaf secara lesu semasa beroperasi.

TABLE OF CONTENTS

LIST OF TABLES

LIST OF FIGURES

LIST OF SYMBOLS

D, d	-	diameter
F	-	Force
G	-	Gravity = 9.81 m/s
I	-	Moment of Inertia
l	-	Length
m	-	Mass
N	-	Rotational velocity
P	-	Pressure
Q	-	Volumetric flow-rate
r	-	Radius
T	-	Torque
ρ	-	Density

LIST OF APPENDICES

CHAPTER 1

INTRODUCTION

1.1 BACKGROUND STUDY

Wastewater lift stations are facilities designed to move wastewater from lower to higher elevation through pipes. Key elements of lift stations include a wastewater receiving well (wet-well), often equipped with a screen or grinding to remove coarse materials, pumps and piping with associated valves , motors, a power supply system, an equipment control & alarm system, an odor control system and ventilation system.

Lift station Equipment and systems are often installed in an enclosed structure. They can be constructed on-site (custom-designed) or prefabricated. Lift station capacities range from 76 liters per minute (20 gallons per minute) to more than 378,500 liters per minute (100,000 gallons per minute). Pre-fabricated lift stations generally have capacities of up to 38,000 liters per minute (10,000 gallons per minute).

Centrifugal pumps are commonly used in lift stations. A trapped air column, or bubbler system, that senses pressure and level is commonly used for pump station control. Other control alternatives include electrodes placed at cut-off levels, floats,

mechanical clutches, and floating mercury switches. A more sophisticated control operation involves the use of variable speed drives.

Lift stations are typically provided with equipment for easy pump removal. Floor access hatches or openings above the pump room and an overhead monorail beam, bridge crane, or portable hoist are commonly used. The two most common types of lift stations are the dry-pit or dry-well and submersible lift stations. In dry-well lift stations, pumps and valves are housed in a pump room (dry pit or dry -well), that is easily accessible.

The wet-well is a separate chamber attached or located adjacent to the dry-well (pump room) structure. Figures 1 and 2 illustrate the two types of pumps;

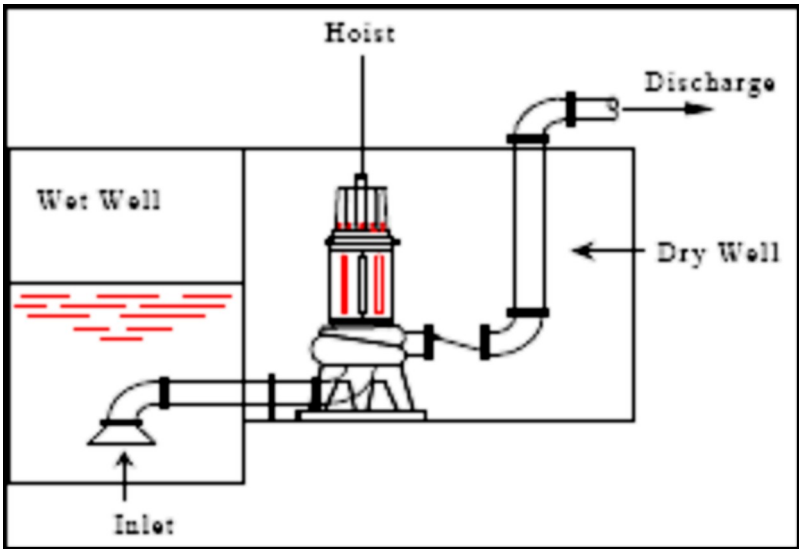

Figure 1.1: Dry well installed pump

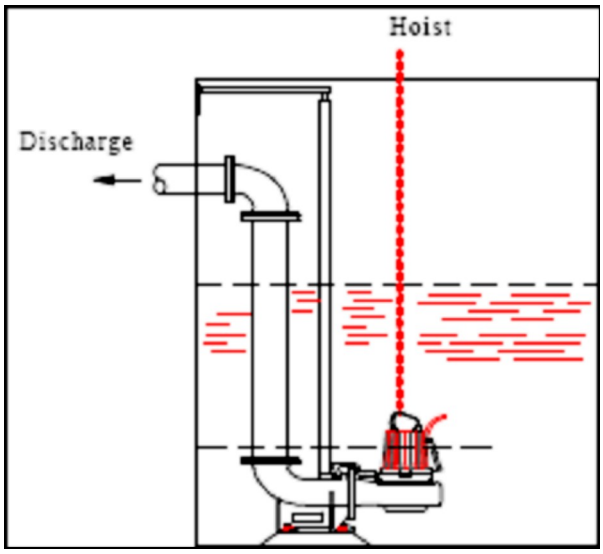

Figure 1.2: Wet well installed pump

The number of wastewater pumps and associated capacity is selected to provide head capacity characteristics that correspond as nearly as possible to wastewater quantity fluctuations. This is accomplished by preparing pump/pipeline system head-capacity curves showing all conditions of head (elevation of a free surface of water) and capacity under which the pumps will be required to operate.

The overall performance of a lift station depends on the performance of the pumps. All pumps have four common performance characteristics: capacity, head, power, and overall efficiency. Capacity (flow rate) is the quantity of liquid pumped per unit of time, typically measured as gallons per minute (gpm) or million gallons per day (mgd) and cubic meter per day (m^3/day).

Head is the energy supplied to the wastewater per unit weight, typically expressed as feet of water or meter. Power is the energy consumed by a pump per unit time, typically measured as kilowatt-hours. Overall efficiency is the ratio of useful hydraulic work performed to actual work input. Efficiency reflects the pump relative power losses and is usually measured as a percentage of applied power.

1.2 PROBLEM DEFINITION

Submersible pump are widely used in a wastewater pumping station and treatment plants, to transfer sewage from a sump or wet well to other parts of the processes. Usually when a centrifugal pump is operating at its best efficiency point (BEP), the bending forces are evently distributed around the impeller. If the pump discharge is throttled from this best efficiency point, then the fluid velocity is changed and causes the hydraulic radial imbalances load to increase at the impeller of the pump.

Therefore, the shaft of the submersible pump is subjected to cyclic stresses due to this hydraulic radial imbalance loading and torsion load. It has been found that there has been frequent failures to the shaft of the submersible pump and is suspected due to fatigue failure caused by this cyclic stresses.

This thesis focuses mainly on the study of the distribution of stresses due to the hydraulic radial imbalance loading, torsion load and fatigue life prediction of the shaft parts. The analysis will be only focusing on a particular model, which has an output of 30 KW.

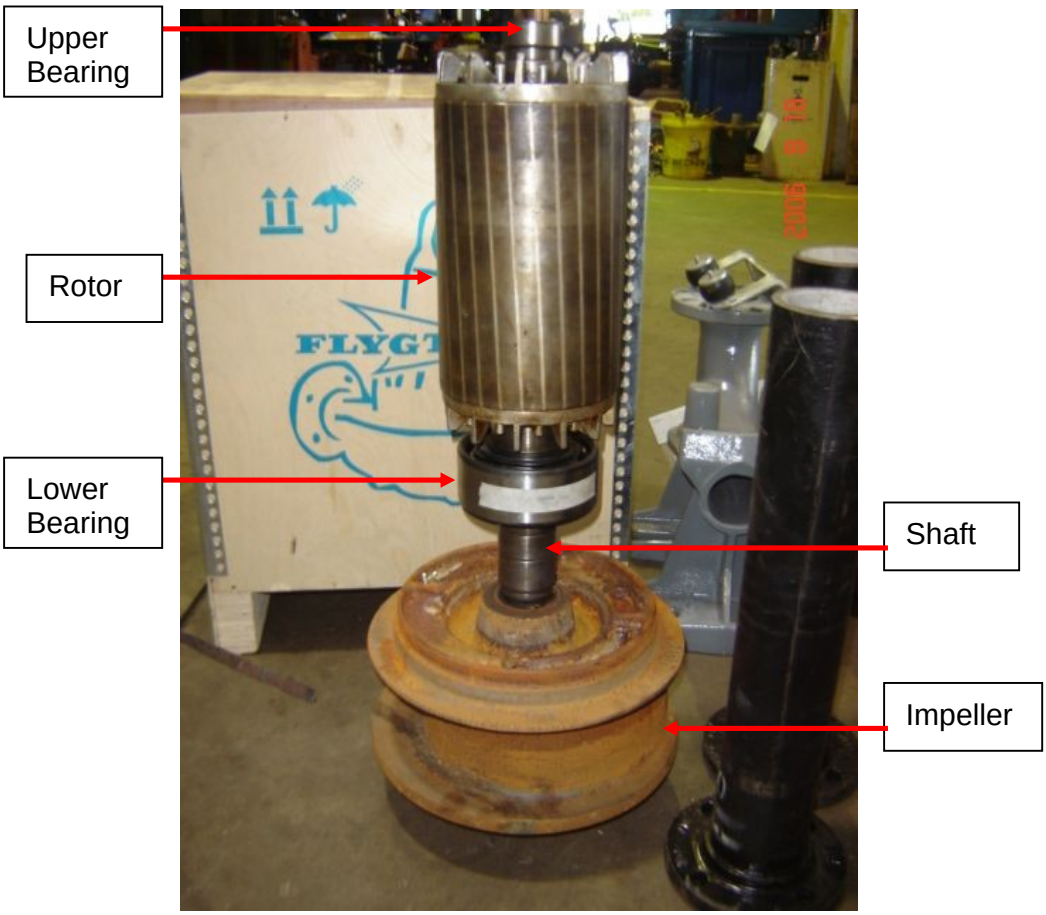

Figure 1.3: Actual Assembly of a submersible pump

Figure 1.4: Failure of shaft

Figure 1.5: Location of the Failure of shaft

1.3 OBJECTIVE & CONTRIBUTION OF THE THESIS

The main objectives of this thesis are stated as per the following;

1. To determine the distribution of stresses in the critical area of the shaft due to the hydraulic radial imbalance loadings.
2. To determine the causes of failure to the pump shaft.

CHAPTER 2

LITERATURE REVIEW

2.1 SHAFTS

The term "shaft" applies to rotating machine members used for transmitting power or torque. The shaft is subject to torsion, bending, and occasionally axial loading. Stationary and rotating members, called axles, carry rotating elements, and are subjected primarily to bending. *Transmission* or line shafts are relatively long shafts that transmit torque from motor to machine. *Countershafts* are short shafts between the driver motor and the driven machine. Head shafts or stub shafts are shafts directly connected to the motor. Motion or power can be transmitted through an angle without gear trains, chains, or belts by using flexible shafting.

Such shafting is fabricated by building up on a single central wire one or more superimposed layers of coiled wire. Regardless of design requirements, care must be taken to reduce the stress concentration in notches, keyways, etc. Proper consideration of notch sensitivity can improve the strength more significantly than material consideration.

Equally important to the design is the proper consideration of factors known to influence the fatigue strength of the shaft, such as surface condition, size, temperature, residual stress, and corrosive environment. High-speed shafts require

not only higher shaft stiffness but also stiff bearing supports, machine housings, etc. High-speed shafts must be carefully checked for static and dynamic unbalance and for first-and second order critical speeds.

The design of shafts in some cases, such as those for turbo pump, is dictated by shaft dynamics rather than by fatigue strength considerations (ref. 2). The lengths of journals, clutches, pulleys, and hubs should be viewed critically because they very strongly influence the overall assembly length. Pulleys, gear couplings, etc., should be placed as close as possible to the bearing supports in order to reduce the bending stresses.

The dimensions of shafts designed for fatigue or static strength are selected relative to the working stress of the shaft material, the torque, the bending loads to be sustained, and any stress concentrations or other factors influencing fatigue strength. Shafts designed for rigidity have one or more dimensions exceeding those determined by strength criteria in order to meet deflection requirements on axial twist, lateral deflection, or some combination thereof. An increase in shaft diameter may also be required to avoid unwanted critical speeds.

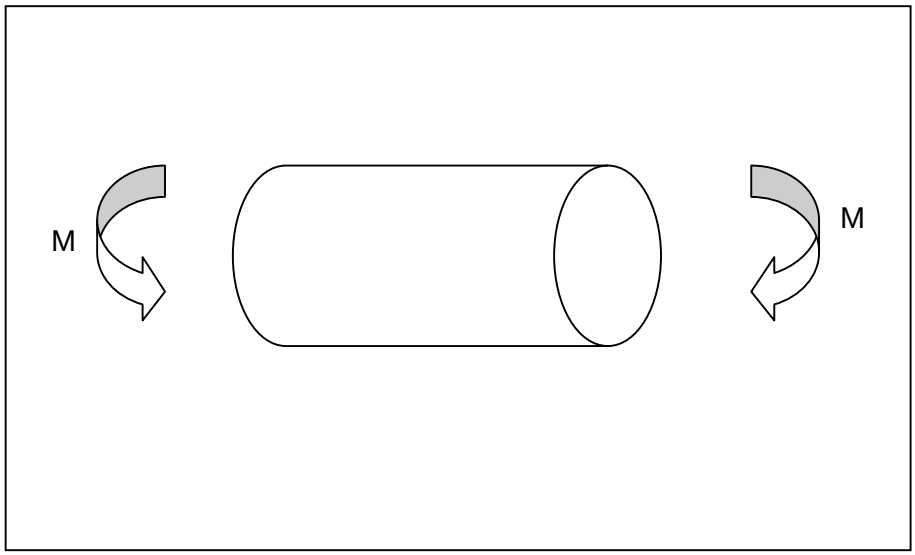

Figure 2.1: Shaft with simple bending

2.2 PROPERTIES OF MATERIAL

Based on the manufacturerôs specification for the shaft material, the following are the material properties as published data;

Material : Carbon Steel, C 1035

A. Chemical Properties

Chemical Composition wt, %

C	0.2
Si	0.5
Mn	1.0 ï 1.6
P	0.05
S	0.3
Cr	0.4

B. Physical Properties

Density	7.85 g/cm3

C. Mechanical Properties

Yield Stress	290 MPa
Tensile strength	490 MPa
Youngôs Modulus	210 GPa
Hardness	165 HB

The actual shaft material has been taken and sent for chemical composition and hardness test at Faculty of Mechanical Engineering, University Teknologi Malaysia, to determine the actual properties of the material used, and to compare with the properties stated as published data.

The comparison between the specification of carbon steel for published and analyzed data are as per the following;

Chemical Composition, %	Published Data	Tested Data
Carbon	0.2	0.135
Si	0.5	0.259
Mn	1.0 ï 1.6	1.49
P	0.05	0.01
S	0.3	0.03
Cr	0.4	0.07

Table 2.1: Chemical Composition of Material

Based on the comparison above, it can be seen that the actual composition of the actual shaft material is way less than a typical carbon steel material properties. Therefore, the actual shaft material can be concluded as Low Carbon Steel as the percentage of carbon is less that 0.2 %.

2.3 FATIGUE

The concept of fatigue is very simple, when a motion is repeated, the object that is doing the work becomes weak. For example, when you run, your leg and other muscles of your body become weak, not always to the point where you can't move them anymore, but there is a noticeable decrease in quality output.

This same principle is seen in materials. Fatigue occurs when a material is subject to alternating stresses, over a long period of time. Examples of where Fatigue may occur are: springs, turbine blades, airplane wings, bridges and bones.

2.3.1 Cyclic Stresses

There are three common ways in which stresses may be applied: axial, torsional, and flexural. There are also three stress cycles with which loads may be applied to the sample. The simplest being the reversed stress cycle . This is merely a sine wave where the maximum stress and minimum stress differ by a negative sign. An example of this type of stress cycle would be in an axle, where every half turn or half period as in the case of the sine wave, the stress on a point would be reversed.

The most common type of cycle found in engineering applications is where the maximum stress (σ_{max})and minimum stress (σ_{min}) are asymmetric (the curve is a sine wave) not equal and opposite. This type of stress cycle is called repeated stress cycle. A final type of cycle mode is where stress and frequency vary randomly.

2.3.2 S-N Curve

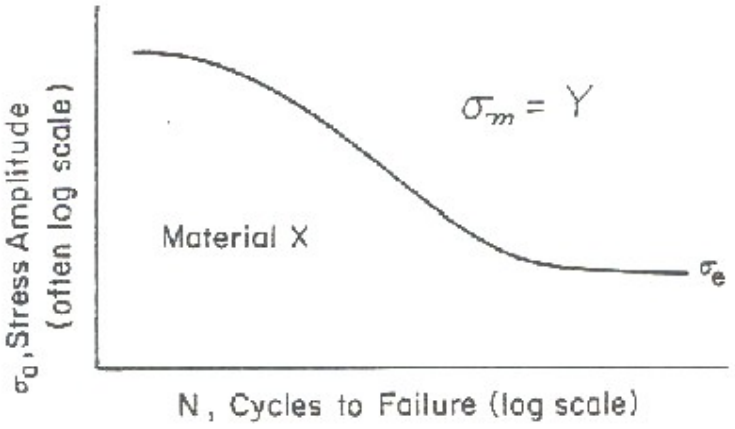

Figure 2.2: Typical S-N Curve for a material

The significance of the fatigue limit is that if the material is loaded below this stress, then it will not fail, regardless of the number of times it is loaded. Material such as aluminum, copper and magnesium do not show a fatigue limit, therefore they will fail at any stress and number of cycles.

Other important terms are fatigue strength and fatigue life. The stress at which failure occurs for a given number of cycles is the fatigue strength. The number of cycles required for a material to fail at a certain stress in fatigue life.

2.3.3 Crack Initiation and Propagation

Failure of a material due to fatigue may be viewed on a microscopic level in three steps:

1. *Crack Initiation:* The initial crack occurs in this stage. The crack may be caused by surface scratches caused by handling, or tooling of the material; threads (as in a screw or bolt); slip bands or dislocations intersecting the surface as a result of previous cyclic loading or work hardening.
2. *Crack Propagation:* The crack continues to grow during this stage as a result of continuously applied stresses
3. *Failure:* Failure occurs when the material that has not been affected by the crack cannot withstand the applied stress. This stage happens very quickly.

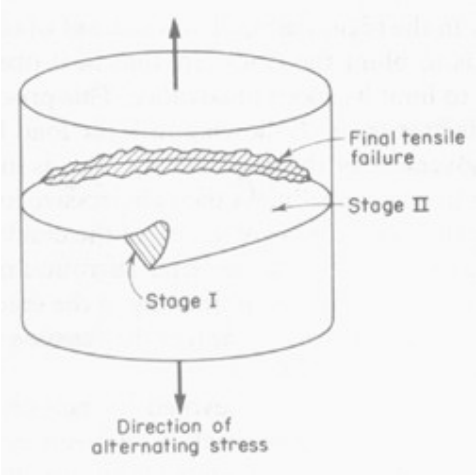

Figure 2.3: Diagram showing location of the three steps in a fatigue fracture under axial stress

2.3.4 Factors That Affect Fatigue Life and Solutions

The Mean stress has the affect that as the mean stress is increased, fatigue life decreases. This occurs because the stress applies is greater. It is mentioned previously that scratches and other imperfections on the surface will cause a decrease in the life of a material. Therefore making an effort to reduce these imperfections by reducing sharp corners, eliminating unnecessary drilling and stamping, shot peening, and most of all careful fabrication and handling of the material.

Another Surface treatment is called case hardening, which increases surface hardness and fatigue life. This is achieved by exposing the component to a carbon-rich atmosphere at high temperatures. Carbon diffuses into the material filling interstisties and other vacancies in the material, up to 1 mm in depth.

Exposing a material to high temperatures is another cause of fatigue in materials. Thermal expansion, and contraction will weaken bonds in a material as well as bonds between two different materials. For example, in space shuttle heat shield tiles, the outer covering of silicon tetraboride (SiB_4) has a different coefficient of thermal expansion than the Carbon-Carbon Composite. Upon re-entry into the earth's atmosphere, this thermal mismatch will cause the protective covering to weaken, and eventually fail with repeated cycles.

Another environmental affect on a material is chemical attack, or corrosion. Small pits may form on the surface of the material, sim ilar to the effect etching has when trying to find dislocations. This chemical attack on a material can be seen in unprotected surface of an automobile, whether it be by road salt in the winter time or exhaust fumes. This problem can be solved by adding protective coatings to the material to resist chemical attack.

2.3.5 Causes and Recognition of Fatigue Failures

General Causes of Material Failures:

- Design deficiencies
- Manufacturing deficiencies
- Improper and insufficient maintenance
- Operational overstressing
- Environmental factors (i.e. heat, corrosion, etc.)
- Secondary stresses not considered in the normal operating conditions
- Fatigue failures

Improper and insufficient maintenance seems to be one of the most contributing factors influenced by some improper designs such as areas that are hard to inspect and maintain and the need for better maintenance procedures. In many circumstances the true load is difficult to predict resulting in a structure being stressed beyond its normal capabilities and structural limitations.

When a structure is subject to cyclic loads, areas subject to fatigue failure must be accurately identified. This is often very hard to analyze, especially in a highly composite structure for which analysis has a high degree of uncertainty. Thus, in general, experimental structural fatigue testing is frequently resorted to.

Two fatigue zones are evident when investigating a fracture surface due to fatigue, the fatigue zone and the rupture zone. The fatigue zone is the area of the crack propagation. The area of final failure is called the rupture or instantaneous zone. In investigation of a failed specimen, the rupture zone yields the ductility of the material, the type of loading, and the direction of loading. The relative size of the rupture zone compared with the fatigue zone relates the degree of overstress applied to the structure.

The amount of overstressing can be determined from the fatigue zone as follows: highly overstressed if the area of the fatigue zone is very small compared with the area of the rupture zone; medium overstress if the size or area of both zones

are nearly equal; low overstress if the area of rupture zone is very small. Figure 8 describe these relations between the fatigues and rupture zones.

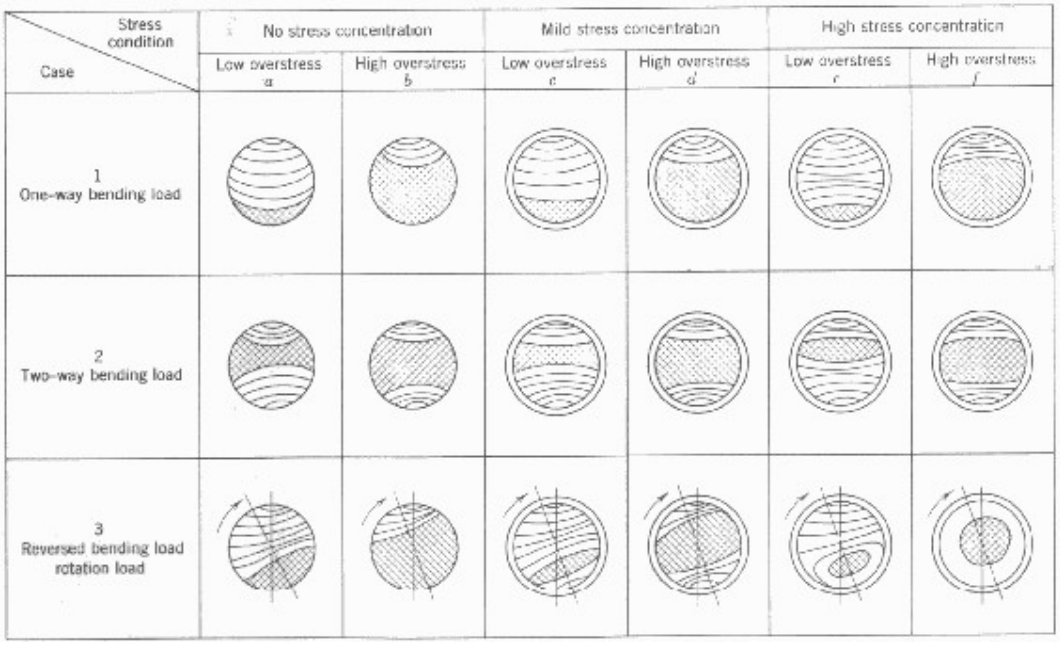

Figure 2.4 : Fracture appearances of fatigue failures in Bending

The fatigue zone can be described as follows: a smooth rubbed, and velvety appearance, the presence of waves known as "clam-shells" or "oyster-shells", "stop marks" and "beach marks," and the herringbone pattern or granular trace which shows the origin of the crack. In general, stop marks indicate the variations in the rate of crack propagation due to variations in stress amplitude in a cyclic application varying with time.

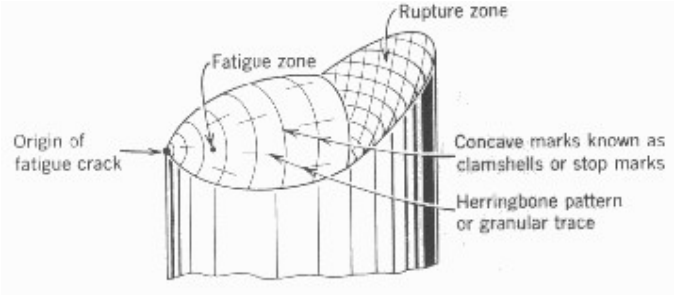

Figure 2.5: Typical fatigue zone with identifying marks

2.3.6 Design Considerations

Even if careful attention to good design practices is constantly the goal of design engineers, fatigue problems are sometimes introduced into the structure. Fatigue failures are often the result of geometrical or strain discontinuities, poor workmanship or improper manufacture techniques, material defects, and the introduction of residual stresses that may add to existing service stresses.

Typical factors affecting fatigue include the following: Stres s raisers, usually in the form of a notch or inclusion; most fatigue fractures may be attributed to notch effects, inclusion fatigue specimens are rare. High strength materials are much more notch-sensitive than softer alloys. Corrosion is another factor that affects fatigue. Corroded parts form pits that act like notches. Corrosion also reduces the amount of material which effectively reduces the strength and increases the actual stress.

Decarburization, the loss of carbon from the surface of the material, is the next factor. Due to bending and torsion, stresses are highest at the surface; decarburization weakens the surface by making it softer. Finally, residual stresses which add to the design stress; the combined effect may easily exceed the limit stress as imposed in the initial design.

2.3.7 Influence of Processing and Metallurgical Factors on Fatigue

A myriad of factors affect the behavior of a material under fatigue loading. Obvious factors include the sign, magnitude, and frequency of loading, the geometry and material strength level of the structure and the ambient service temperature. However, processing and metallurgical factors are not often considered, but these factors determine the homogeneity of materials, the sign and distribution of resi dual stresses, and the surface finish. Thus, processing and metallurgical factors have an overriding influence on the performance of a structure.

A. Processing Factors

Stresses are normally highest at the surface of a structure, so it follows that fatigue usually initiates at the surface. Stress raisers are more likely to be present as a result of surface irregularities introduced by the design of the structure or produced in service or resulting from processing. Processing factors can introduce a detrimental or beneficial effect into a structure, usually in the form of effect on strength level or residual stress condition of the surface material. Therefore, the effect of processing on the mechanical properties of a material, especially the surface of the material, directly affects fatigue properties.

Processing factors that influence the fatigue life of a structure include the following: the process by which a part is formed, such as die casting; the heat treatment of a material, such as quenching, which builds up residual stresses and annealing, which relieves internal stress (see Figure 3); case hardening, such as carburization or nitriding, which increases surface hardness and strength (see Figure 4); surface finish, such as polished smooth by electro polishing; cold working, which increases strength; also, cladding, plating, chemical conversion coatings.

B. Metallurgical Factors

Metallurgical factors refers to areas within the material, either on the surface or in the core, which adversely affect fatig ue properties. These areas may arise from melting practices or primary or secondary working of the material or may be characteristic of a particular alloy system. In virtually all instances the detriment to fatigue properties results from a local stress-raising effect.

Therefore, metallurgical factors affecting fatigue include the following: surface defects, sub-surface and core defects, inhomogenity, anisotropy, improper heat treatment, localized overheating, corrosion fatigue, and fretting corrosion.

CHAPTER 3

ABAQUS

3.1 INTRODUCTION

The Abaqus suite of software for finite element analysis consists of three main products;

- Abaqus / Standard
- Abaqus / Explicit
- Abaqus / CAE

The standard package solves static, dynamic and thermal problems. The explicit package focus on transient dynamics and quasi-static analysis. The CAE package is CAD like tool to create models for analysis and for visualization of results.

In this thesis, the models has been created in Abaqus / CAE and analysis package used in Abaqus / Standard, hence all analysis are static.

3.2 CREATING MODELS

The CAE package is using different modules. These modules are used in order they are presented so the models are created with the same procedure.

- Part Module : The parts are created using Graphical User Interface (GUI)
- Property Module: All the material properties are given such as elastic and plastic behaviour. The orientation of the beam, etc, is given.
- Assembly Module: The parts are imported to create the geometry of the model, i.e to build the complete structure.
- Step Module: This module decides which type of analysis that is going to be used. The analysis is divided into one or more steps. These steps capture the changes in the model. Here are the output requests defined. There are two different procedures for the step;
    - General ï These steps define sequential events. The state of the model at the end of one general steps.
    - Linear Perturbation ï These steps provide the linear response of the model about the state reached at the end of the last general non linear steps.
- Interaction Module: Here all the relationships between the parts defined.
- Load Module: In this module, all the loads and boundary conditions are defined. The loads are step-dependent.
- Mesh Module: This module generates meshes on the assemblies. One part can be divided into three different meshes and different element too.
- Job Module: The jobs are created and submitted for analysis. It is possible to submit and write only input files for latest usage.
- Visualization Module: The results of the analysis can be visualized in this module. It is possible to make different plots at selected.

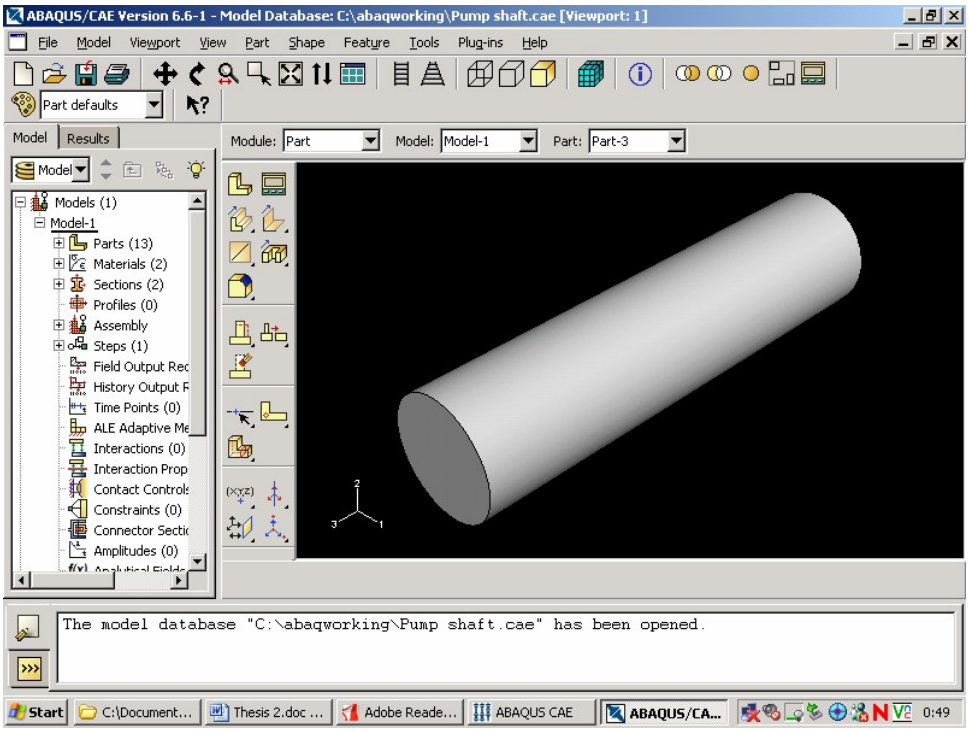

Figure 3.1: Abaqus standard environment

3.3 ELEMENTS

Abaqus offers a variety of elements. The analysis in this thesis uses solid elements as the main featured elements. There are basically four different types of elements; shell element, solid element, beam element and rigid elements.

3.3.1 Shell Element

Abaqus has three categories of shell elements; general purpose, thin and thick shell elements. Thin elements provide solutions to shell problems that are adequately described by classical shell theory, thick shell elements yield solutions for structures that are best modeled by shear flexible shell theory, and general purpose structures shell element can provide solutions to both thin and thick shell problems.

The general purpose shell elements are axisymmetric elements and three dimensional elements. The general purpose elements provide robust and accurate solutions in all loading conditions for thin and thick shell problems.

Thin elements may provide enhance performance for large problems where reducing the number of degrees of freedom through the use of five degree of freedom shells is desirable. While the thick elements has non negligible transverse shear flexibility as required by these elements to function properly.

3.3.2 Solid Elements

Solid elements are provided with first order (linear) and second order (quadratic) interpolation. Standard first order elements are essentially cons tant strain elements. The second order elements are capable of representing all possible linear strain fields. Thus, in the case of elliptic problems, much higher solution accuracy per degree of freedom is usually available with the higher order elements.

For elliptic applications, second order elements are preferred. Though the accuracy per degree of freedom is higher, the accuracy per computational cost may not be increasing. Abaqus does not include elements beyond second order. Practical experience suggests that little is gain with those elements.

With a fixed mesh that does not use special element that admits discontinuities in their formulations, the first order elements are likely to be most successful. For a given number of nodes, they provide the most locations at which some component of the gradient of the solutions can be discontinuous.

Thus, element C3D8R which is a solid 8 node linear brick with three degree of freedom per node. In corners and complicated parts, the element C3D4 is used. It is a 4 node linear tetrahedron with three degree of freedom at each node. All the solid elements in Abaqus are written to include finite strain effects.

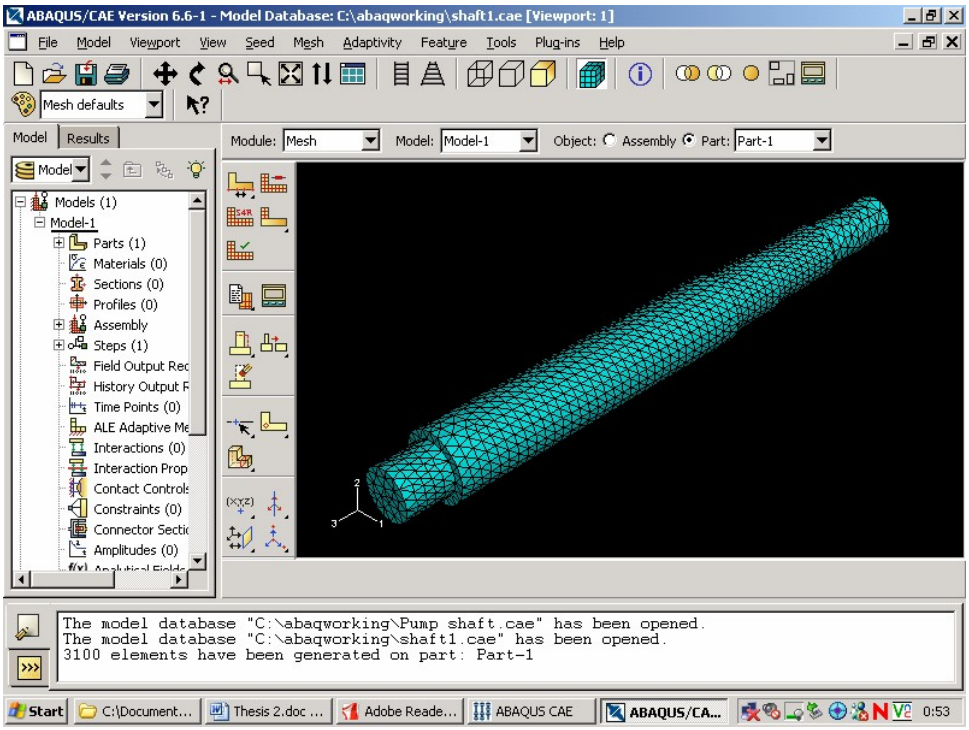

Figure 3.2: Meshing with solid elements

3.3.3 Beam Element

A beam in this context is an element in which assumptions are made so that the problem is reduced to one dimensional mathematically. The simplest approach to beam theory is the classical Euler-Bernoulli assumption. The beam element that uses cubic interpolation also uses this assumption.

This approximation can also be used to formulate beams for large axial strains as well as large rotations. The beam element in Abaqus that use linear and quadratic interpolation, are based on such a formulation, with the addition that these elements also allow transverse shear strains.

This extension leads to Timoshenko beam theory. The large strain formulation in these elements allows axial strain of arbitrary magnitude, but quadratic terms in the nominal torsional strain is neglected compared to unity, and the axial strain is assumed to be small in the calculation of the torsional shear Strain.

3.3.4 Rigid Elements

Rigid elements are associated with a given rigid body and share a common node known as the rigid body reference node. A rigid element can be used t o define the surfaces of rigid bodies for contact or to define rigid bodies for multi body dynamic simulations. They also be attached to deformable elements or be used to constraint parts of a model. The rigid element used is usually four node elements in three dimensional.

CHAPTER 4

FE- SAFE

4.1 INTRODUCTION

FE-SAFE is an advanced easy-to-use suite of durability analysis software which interfaces to finite element models. FE-SAFE combines component loading, FEA stresses, and materials data, and performs advanced multiaxial fatigue analysis. Fatigue hot-spots are automatically identified. 3-D contour plots can be displayed for fatigue life and for allowable stress factors for a specified design life.

FE-SAFE can be used for re-design and ówhat-ifô analysis, for the whole model or for selected areas, to investigate the effect of removing metal from non-critical regions and to increase the life at hot-spot locations of temperature, surface finish, notch sensitivity, geometry changes, and changes in material properties and service duty can be investigated quickly. Designs can be optimized rapidly, material costs are reduced, and the final design can be verified on the computer, giving more confidence that the design will pass test schedules as right-first-time.

FE-SAFE was developed under a $1million project in collaboration with Rover Group. Extensive tests on real components were used to develop the software. FE-SAFE interfaces to many FEA suites and post -processors, including ABAQUS, ANSYS, FEMSYS, IDEAS, Pro/Engineer, Pro/Mechanica, Hypermesh and FAM.

The ABAQUS interface reads and writes to the .fil file and the new ABAQUS/CAE database available with ABAQUS 6.4.1.

A CATIA and a NASTRAN interface will be released later this year. FE-SAFE is supported on Silicon Graphics, Hewlett Packard and Sun UNIX workstations, and will be available on PCôs running Windows NT. Continuing research projects and customer-specified developments are being used to ensure that FE-SAFE remains at the forefront of engineering durability by design.

4.2 AN OVERVIEW OF FE-SAFE

FE-SAFE consists of a user interface, a materials database management system, and fatigue analysis programs.

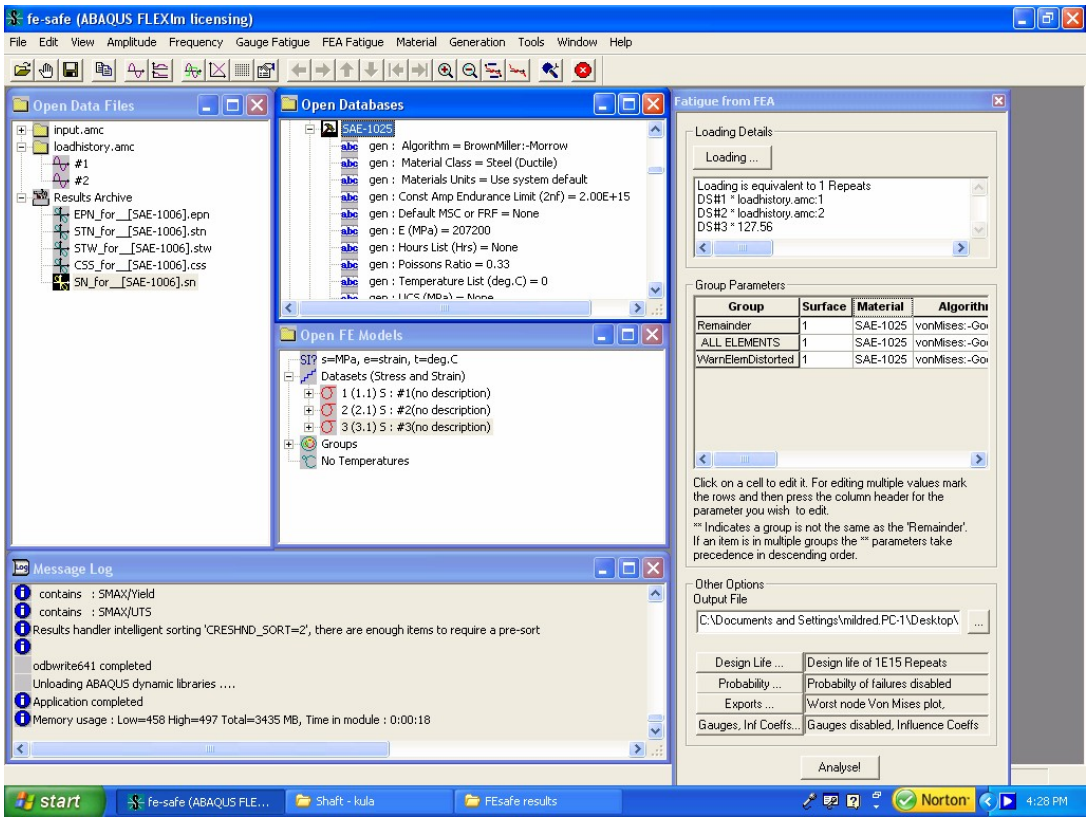

Figure 4.1: Interface of FE-safe

4.2.1 FEA stresses

- Are usually elastic stresses, so that the results can be scaled and superimposed to
  produce service stress time histories.
- Elastic-plastic stresses can be analyzed for certain types of loading.

4.2.2 Component loading

- A time history of component load can be applied to a set of FEA stresses.
- Time histories of multi-axis loading can be superimposed to produce a time history of the stress tensor at each location on the model.
- A sequence of FEA stresses ï for example, the results of a transient analysis, or the analysis of several rotations of an engine crankshaft, or models of several discrete loading conditions, can be analyzed.
- A combination of the above 2 items.
- Block loading programs, consisting of blocks of constant amplitude cycles, can be produced and analyzed.

4.2.3 Materials data

- A comprehensive data base of materials properties is provided.
- The database can be extended and modified by the customer.
- Test reports and background data can be accessed using in-built Netscape links.
- The database is accessed by FE -SAFE during the fatigue analysis set-up and materials data is transferred into the analysis programs. The database may also be accessed directly through the FE-SAFE user interface, to enter new data for example.

4.2.4 Additional factors

- Nodal temperatures can be used to modify materials fatigue properties.
- Effects of surface finish can be included for all or part of the component allowing machined and as-forged surfaces to be differentiated.
- Notch sensitivity effects can be included ï important for cast irons, and some aluminium alloys and lower strength steels (in Release 3.1).
- A design life may be specified.
- The fatigue analysis can be for the complete model, or for an element group.
- Different materials data or stress concentration factors can be used for each element group (to allow for machined and as-forged surfaces on the same component, for example)

4.2.5 Analysis

- Uniaxial analysis using stress-life curves - Goodman, Gerber or no mean stress correction.
- Uniaxial analysis using strain-life curves ï Morrow, Smith-Watson-Topper or no mean stress correction.
- Biaxial fatigue analysis using local stress-strain analysis (maximum shear strain, maximum direct strain, Brown-Miller combined shear and normal strain) implemented as critical plane procedures.
- Von Mises stress.
- Analysis of welded structures using the stress-life data from BS7608.

4.2.6 Output

- FE-SAFE writes output files of nodal fatigue lives. If a design life has been specified, FE-SAFE calculates the stress factor which could be applied at each node to achieve this life. Both of these files can be displayed as 3-D contour plots.
- A list of the most damaged elements is saved, and re-analysis can be concentrated on these elements if required.

- A text file of user inputs, analysis type, program version numbers and a results summary, is produced.

4.2.7 Re-analysis

- The user may change any of the inputs and re-run the analysis.
- FE-SAFE reloads all the previous input parameters when the program is re-run.

4.2.8 Utilities

- Plots of materials data and load histories.
- Importing ASCII and other standard format data files.
- Preparation of single and multi-channel load histories ï scaling, peak/valley with cycle omission.

4.3 FATIGUE ANALYSIS ALGORITHM

The following fatigue damage algorithms are included.

Uniaxial stress ï life

$$\sigma_a = \sigma_f' (2N_f)^b$$

Strain life for Uniaxial stress

$$\varepsilon_a = (\sigma_f' / E)(2N_1)^b + \varepsilon_f' (2N_f)^c$$

Direct strain

$$\varepsilon_1 / 2 = (\sigma_f' / E)(2N_f)^b + \varepsilon_f' (2N_f)^c$$

Von Mises Strain

$$\Delta\varepsilon_{eff}/2 = (\sigma_f'/E)(2N_f)^b + \varepsilon_f'(2N_f)^c$$

4.4 A SINGLE LOAD HISTORY ON A COMPONENT

The FEA file would be an elastic analysis for a unit load. FE -SAFE allows a scale factor to be applied to the loading if the FEA stresses are for a non-unit load. For each node, FE-SAFE calculates a time history of the 6-stress tensor by multiplying the unit load stress tensor by the time history of the load.

If the load case for the FE data set is a load *PFE ,* and for this load the elastic stress at the node is *SFE* . If the loading to be analysed is a load time-history *P(t)*, and one data point in *P(t)* is a value *PK* then the elastic stress at the node *SK = SFE*

A time history of the principal stresses in the plane of the element is calculated. The multiaxial Neuberôs rule is used to calculate the elastic-plastic stresses and strains which result from any cyclic yielding, using a material memory algorithm. The cyclic stress-strain curve is calculated for the biaxial stress condition at the node. If the user has specified an additional stress concentration factor, its effect is included at this stage.

For a single load history the principal stresses at the node do not change direction, so a single fatigue analysis is performed. In this, the shear or direct strains are rainflow cycle counted and the fatigue damage for each cycle is calculated. Minerôs rule is used to calculate the fatigue life at the node.

If a design life has been specified, the program uses an iteration procedure to calculate the factor which could be applied to the stresses in order to achieve the design life.

4.5 MULTIPLE LOAD DIRECTIONS ON A COMPONENT

For each loading direction, the FEA file would contain the results of an elastic analysis for a unit load. FE-SAFE takes the 6-stress tensor for one unit load, and multiplies it by the time history of this load. FE-SAFE then takes the 6-stress tensor for the second unit load, multiplies it by the time history of this load to form a time history of the stress tensor, and adds the time history obtained from the first load.

This is repeated for each load, to create a time history of the stress tensor for all the loads or a stress data set, each of the elastic stresses at the node will be given by an equation of the form

$$S = (S_{FE})_P(P/P_{FE}) + (SFE)_Q(Q/Q_{FE})$$

Where, S - Instantaneous value of one six stresses

PFE - Load used for FE Data set

SFE - Elastic stress at the node for load PFE

P - Instantaneous value of rod P(t) in load time history

QFE - Load used for 2nd FE Data set

Q - Instantaneous value of load Q(t) in load time history

The multiaxial Neuberôs rule is used to calculate the elastic-plastic stresses and strains which result from any cyclic yielding. The cyclic stress-strain curve is re-calculated for the biaxial stress condition for each event in the stress history, using a material memory If the user has specified an additional stress concentration factor, its effect is included at this stage.

For multiple load directions, the principal stresses at the node may change direction during the load history, so a critical plane fatigue analysis is performed. On each plane, the shear or direct strains are rainflow cycle counted and the fatigue damage for each cycle is calculated. Minerôs rule is used to calculate the fatigue life at the node.

The shortest fatigue life on any plane is taken as the fatigue life at the node. If a design life has been specified, the program uses an iteration procedure to calculate the factor which could be applied to the stresses in order to achieve the design life.

4.6 DATA SET SEQUENCE

A data set sequence may be the result of a transient analysis. It may also be created by modeling a series of discrete events, for example the stresses in an engine crankshaft calculated at each 50 of rotation of the crankshaft through (say) four crankshaft revolutions. The calculated stresses at each angle are termed a ódata setô. The data set sequence is specified in a data set sequence file, which allows the sequence of the data sets to be specified, and allows a scale factor to be applied to any data set.

A different scale factor may be applied to each data set (positive or negative), and data sets may appear more than once in the sequence. At each node FE-SAFE creates a time-history of the stress tensor from the sequence of data sets. This is converted into elastic-plastic stress/strain and a critical plane fatigue analysis is used to calculate the fatigue life. Again, a design life may be specified.

4.7 BLOCK LOADING ANALYSIS

Block loading fatigue tests are commonly used. FE-SAFE can simulate block-loading sequences. The user creates a unit load FEA data set for each load condition. For each data set the user may specify two scale factors and a number of cycles. For example, the stresses in data set 1 may be scaled by +1 and +0.1 to create a stress cycle, and the user may specify 1000 cycles of this loading.

This forms one block in the block loading sequence. At present up to 64 blocks may be specified. Data sets may appear more than once in the sequence. FE-SAFE calculates the fatigue damage for each block, and the fatigue damage caused by the transition from block to block. Critical plane analysis is used. Again, a design life may be specified.

CHAPTER 5

PRELIMINARY ANALYSIS OF SHAFT

5.1 SECTIONAL VIEW OF PUMP SHAFT

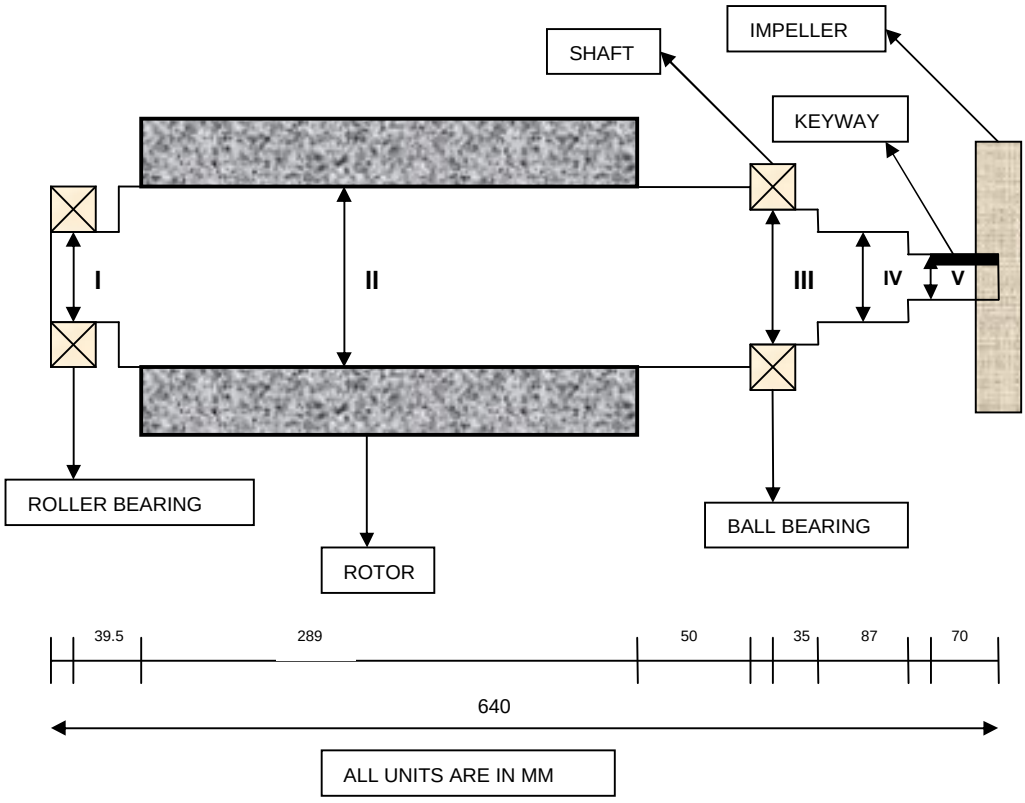

Figure 5.1: Sectional view of pump shaft

Diameter of shaft at various sections is as per the following;

I - 54.00 mm

II - 72.10 mm

III - 63.45 mm

IV - 57.68 mm

V - 49.03 mm

5.2 LOADINGS ON PUMP SHAFT

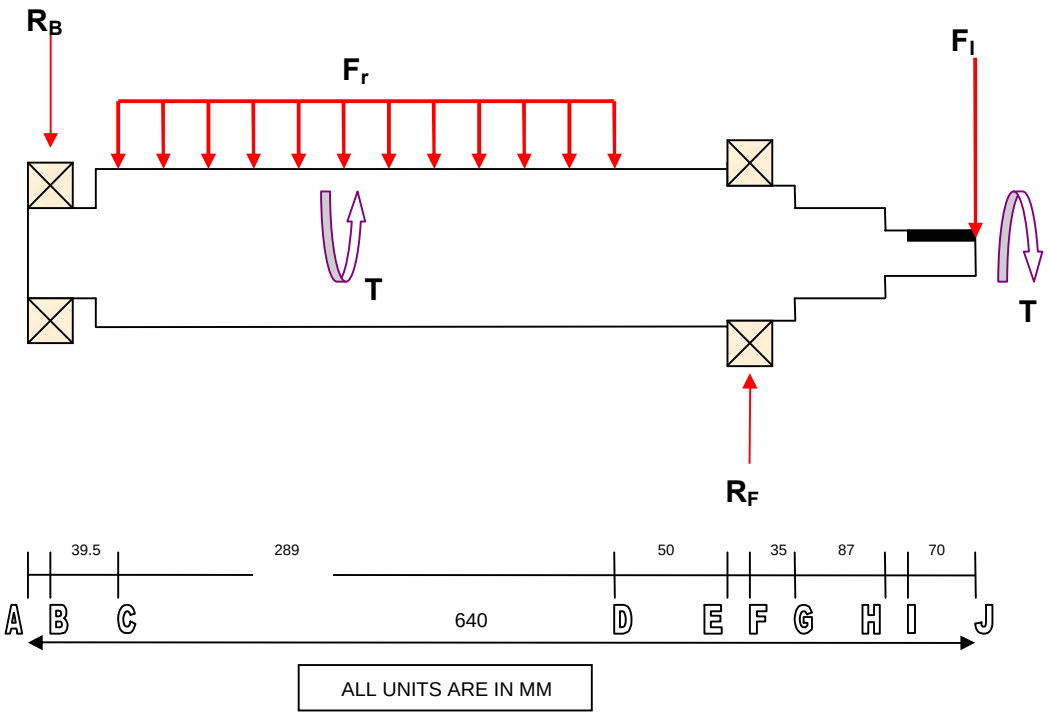

Figure 5.2: Loadings on the pump shaft

Where, the forces are defined as per the following;

F_R = Rotor Loading

F_I = Impeller Loading

R_B = Reaction Load at roller bearing

R_F = Reaction Load at ball bearing

T = Shaft Torque

5.3 PUMP SHAFT LOADING CALCULATIONS

5.3.1 Impeller Loading, F_I

Basically, the loading at the impeller comprises of the following ;

1. Hydraulic Radial Imbalance force
2. Force due the weight of Impeller

The hydraulic radial force is Imbalance forces due to the operation of the pump away from the best efficiency point. The amount of imbalance forces generated at the impeller is calculated using the following formula;

$$P = \frac{K_q \times K \times H \times S.G \times D \times B_2 \times 9.81}{10.2}$$

where,

K = Radial Thrust factor

S.G = Specific gravity of the pumped liquid

H = Total head at BEP (m)

B_2 = Width of impeller including shrouds (cm)

D = O.D of impeller (cm)

while K_q is defined as,

$$\mathbf{K_q = 1 \quad (Q^2/Q_n^2)^2}$$

where,

Q = Actual pumping capacity (m^3/hr)
Q_n = BEP pumping capacity (m^3/hr)

Therefore,

K = 0.25 (given for closed impeller)
S.G = 0.72 (for sewage application)
H = 27.6 m (taken from the pump performance curve)
B_2 = 7.84 cm (taken from the manufacturers specifications)
D = 30 cm (taken from the manufacturers specifications)

Assumption :

$Q / Q_n = 0.9$

Kq = 1 ï $(Q / Q_n)^4$
= 1 ï 0.9^4
= <u>0.344</u>

Hydraulic Imbalance force becomes,

$$F_{imb} = P = \frac{K_q \times K \times H \times S.G \times D \times B_2 \times 9.81}{10.2}$$

$$= \frac{0.344 \times 0.25 \times 27.6 \times 0.72 \times 30 \times 7.84 \times 9.81}{10.2}$$

$$= \mathbf{386.59\ N}$$

Load due to the weight of the impeller is given by;

Moment Inertia of Impeller = 0.38 kgm^2

Diameter of impeller = 300 mm

Area, A = ´ d^2 /4

= (3.142 x 0.3^2)/4

= 0.070695 m^2

Therefore, weight of impeller = I / A

= 0.38 / 0.070695

= 5.38 kg

Load due to weight of impeller = mg

= 5.38 x 9.81

= **52.78 N**

Impeller Loading, F_I = F_{imb} + F_{weight}

= 386.59 + 52.78

= **439.37 N**

5.3.2 Rotor Loading, F_R

Moment Inertia of rotor = 0.539 kgm^2

Diameter of rotor = 181.6 mm

Length of rotor = 289 mm

Area, A = ´ d^2 /4

= (3.142 x 0.1816^2)/4

= <u>0.0259 m^2</u>

Therefore, weight of rotor = I / A

= 0.539 / 0.0259

= <u>20.81 kg</u>

Distributed Load of rotor = mg/L

= (20.81 x 9.81)/0.289

= **<u>706.4 N/m</u>**

5.3.3 Reaction Force at bearings R_B & R_F

Taking equilibrium condition;

$\sum F^{\uparrow +} = \sum F^{\downarrow}$

$R_F = R_B + 439.37 + (706.4 \times 0.289)$

$R_F - R_B = 439.37 + 204.15$

$R_F - R_B = 643.52$ ---------- (1)

$\sum \mathbf{M^B}$ **= 0**

R_F x 0.4085 = (706.4 x 0.3285 x 0.3285/2) ï (706.4 x 0.0395 x 0.0395/2) + (439.37 x 0.629)

0.4085 R_F = 38.11 ï 0.55 + 276.36

0.4085 R_F = 313.92

R_F = 313.92 / 0.4085

R_F = **768.47 N**

Therefore,

R_F - R_B = 643.52

- R_B = 643.52 - R_F

- R_B = 643.52 ï 768.47

- R_B = - 124.95

R_B = **124.95 N**

* Shaft Torque is given by the manufacturer = **200 Nm**

5.4 STATIC ANALYSIS OF PUMP SHAFT

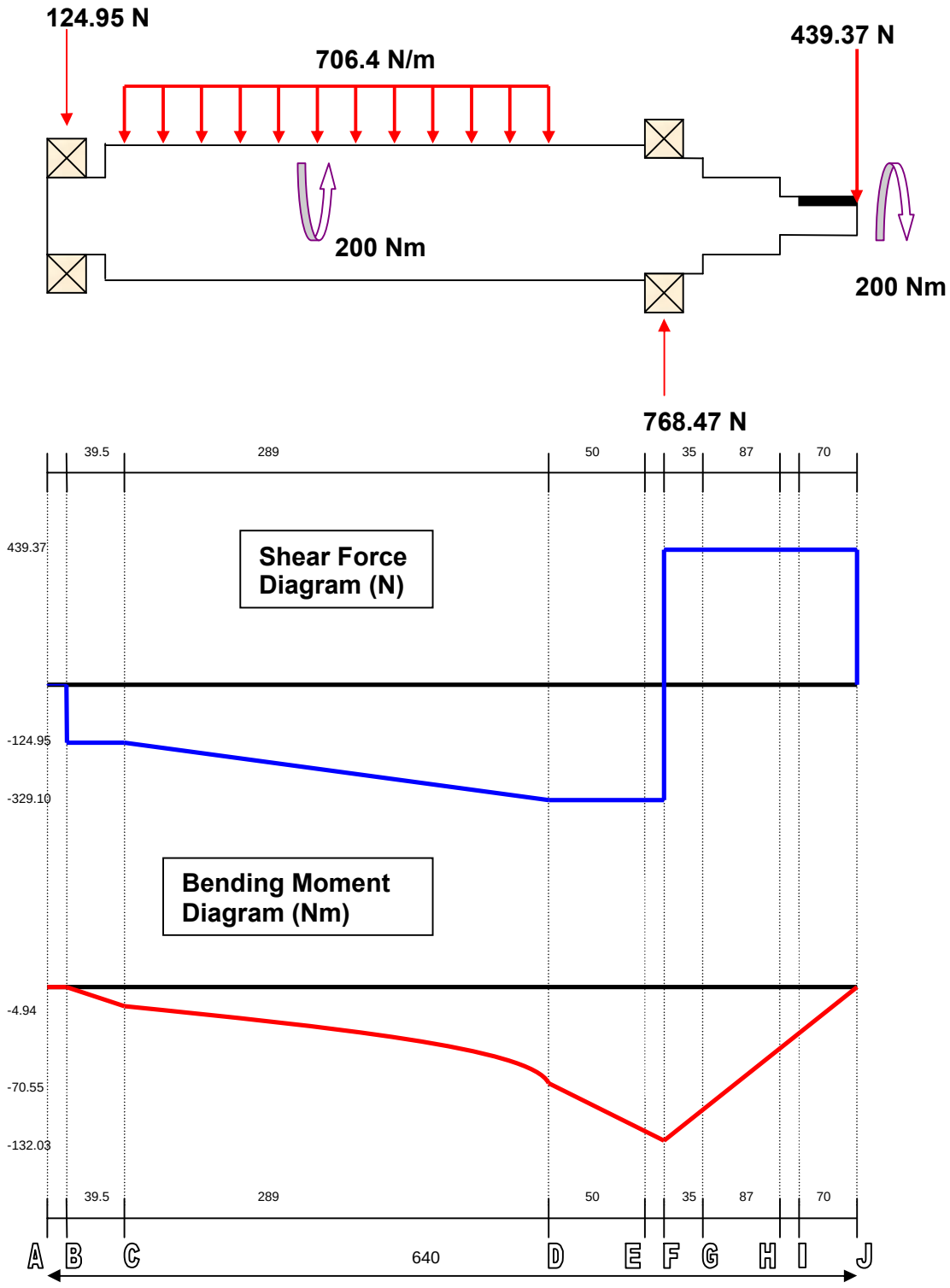

Figure 5.3: Static Analysis of Pump Shaft

5.5 FATIGUE ANALYSIS OF PUMP SHAFT

The submersible pumpôs shaft is made from Low Carbon steel. The designed material properties are as below;

Youngôs Modulus, E	=	210 GPa
Rigidity Modulus, G	=	80 GPa
Ultimate Strength, S_t	=	490 MPa
Yield Strength, S_y	=	290 MPa

Endurance limit for Mechanical element is defined as;

$$\mathbf{S_e = K_a K_b K_c K_d K_e S_e'}$$

Where,

K_a - Surface factor

K_b - Size factor

K_c - Load factor

K_d - Temperature factor

K_e - Fatigue strength reduction factor

S_eô - Endurance limit or fatigue limit

As for the pump shaft;

Endurance limit, is defined as $\mathbf{S_e' = 0.504\ S_t}$ (for steels with S_t Ò1400 MPa)

Therefore,

S_eô$= 0.504\ S_t$

$= 0.504\ (490)$

$= \underline{246.96\ \text{MPa}}$

- Surface factor, $\mathbf{K_a = aS_t^b}$

For a machined steel, the value a & b is given as ;

a = 4.51 MPa & **b = -0.265**

(based on table 7.4 from Shigley/Mischke : Mech. Eng. Design,5th Edition)

$$K_a = aS_t^b$$
$$= 4.51 \times 490^{-0.265}$$
$$= \underline{0.874}$$

- Size factor, K_b is given as 0.60 to 0.75 for bending problems (size larger than 51 mm in diameter).

Therefore, the size factor is assumed to be 0.75.

$$K_b = \underline{0.75}$$

- Load factor, K_c is given as 1.0 for bending problems.

$$K_c = \underline{1.0}$$

- Temperature factor, K_d is given as 1.0 for temperature up to 50^oC.

$$K_d = \underline{1.0}$$

Based on the bending moment diagram, the location with suspected high stress concentration are location F, G, H & I. therefore, the fatigue life analysis will be carried out on these locations.

5.6 SUMMARY OF PRELIMINARY ANALYSIS OF SHAFT

Location	D (mm)	d (mm)	r (mm)	D/d	r/d	K_t	Q	K_f	K_e	S_e (MPa)
F	72.10	63.45	3	1.14	0.05	2.05	0.78	1.819	0.55	89.04
G	63.45	57.68	3	1.10	0.05	1.95	0.78	1.741	0.574	92.92
H	57.68	49.03	3	1.18	0.06	1.95	0.78	1.741	0.574	92.92
I	57.68	49.03	3	1.18	0.06	1.79	0.78	1.6162	0.619	100.21

Table 5.1: Fatigue limit , S_e, calculated data for different locations on the shaft

Location	B. Moment (Nm)	B. Stress (σ_a)	a	b	Estimated Life cycle, N
F	132.03	5.27	2426.89	-0.2316	**3.16×10^{11}**
G	111.09	5.90	2325.55	-0.2254	**3.28×10^{11}**
H	58.99	5.10	2325.55	-0.2254	**6.26×10^{11}**
I	41.92	3.62	2156.37	-0..2145	**8.65×10^{12}**

Table 5.2: Fatigue Life cycle for critical area on shaft

Based on the results obtained through fatigue analysis (calculation) as per Table 5.1 & 5.2, it can be seen that the shaft has been designed to infinite life where the life cycle of all the critical locations are > 10^6 cycles. Besides that, it is also noted that the location with the highest bending stress is location G, which is a stress raiser due to the surface discontinuity as there is a diameter step down after the ball bearing. The location where the shaft actually failed has been found to have infinite life as well as the life is 10^{12} cycles.

Location	Bending stress, σ_a	Shear stress, T_{xy}	Principle Stresses (MPa)		Von Mises Stress, σ'	Safe Factor, n
	MPa	MPa	σ_A	σ_B	MPa	
F	5.27	3.99	7.417	-2.15	8.69	10.25
G	5.90	5.31	9.02	-3.12	10.92	8.51
H	5.10	8.64	11.56	-6.46	15.81	5.88
I	3.62	8.64	10.64	-7.02	15.40	8.11

Table 5.3: Distribution of stresses at critical area on the shaft

Based on the table 3 as above, it can be seen that the von Mises stress is high at locations H & I. But the stresses are still way below the endurance limit of the part of the shaft respectively. Therefore, failure due to fatigue will not occur.

CHAPTER 6

3-D SHAFT ANALYSIS

6.1 FINITE ELEMENT ANALYSIS

6.1.1 Modeling of shaft

The submersible pump shaft was m odeled using existing commercial FEA software, ABAQUS. The dimensions or size of the shaft modeled was to the exact dimensions of the shaft that has failed in practical use.

There are two (2) boundary conditions for the shaft, which is at the location where the shafts are supported by its upper and lower bearings. The details of the boundary conditions are as follows;

Boundary Condition 1 : Upper bearing (Thrust bearing)
U1 = 0, U2 = 0, U3 = 0
UR1 = 0, UR2 = 0

Boundary Condition 2 : Lower bearing (Ball bearing)
U1 = 0, U2 = 0, U3 = 0
UR1 = 0, UR2 = 0

Where,

1. U1, U2 & U3 are the displacements in x, y and z axis.
2. UR1, UR2 & UR3 are the rotational displacements at x, y and z axis.

The 3D model of shaft in ABAQUS and its boundary conditions are shown in the following figure;

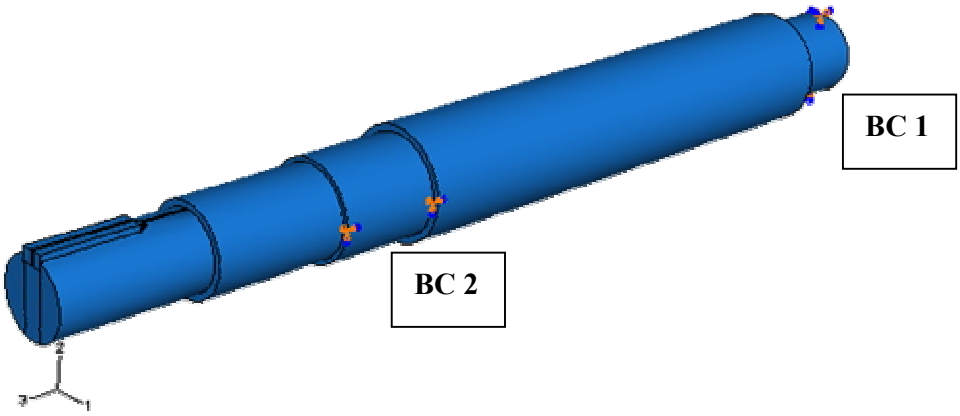

Figure 6.1: 3D Model and Boundary conditions on a shaft

6.1.2 Loadings on Shaft

The shaft basically goes through the following loadings during in operation;

- Lateral loading due to weight of the impeller and hydraulic imbalance load.
- Tangential load due to the torque from the motor of the pump.

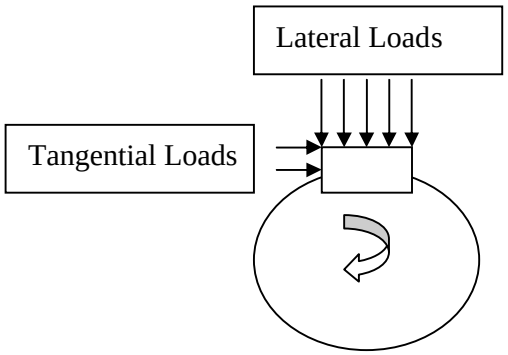

Figure 6.2: Types of loading on a shaft

A. Lateral Loading

F_{imb} = 386.59 N

F_{weight} = 52.78 N

Total Loadings = F_{imb} + F_{weight}

= 386.59 + 52.78

= **439.37 N**

Effective area of loading = 63 mm x 14 mm

= **882 mm^2**

Therefore, pressure = Force / Area

= 439.37 / 882

= **0.498 N/mm^2**

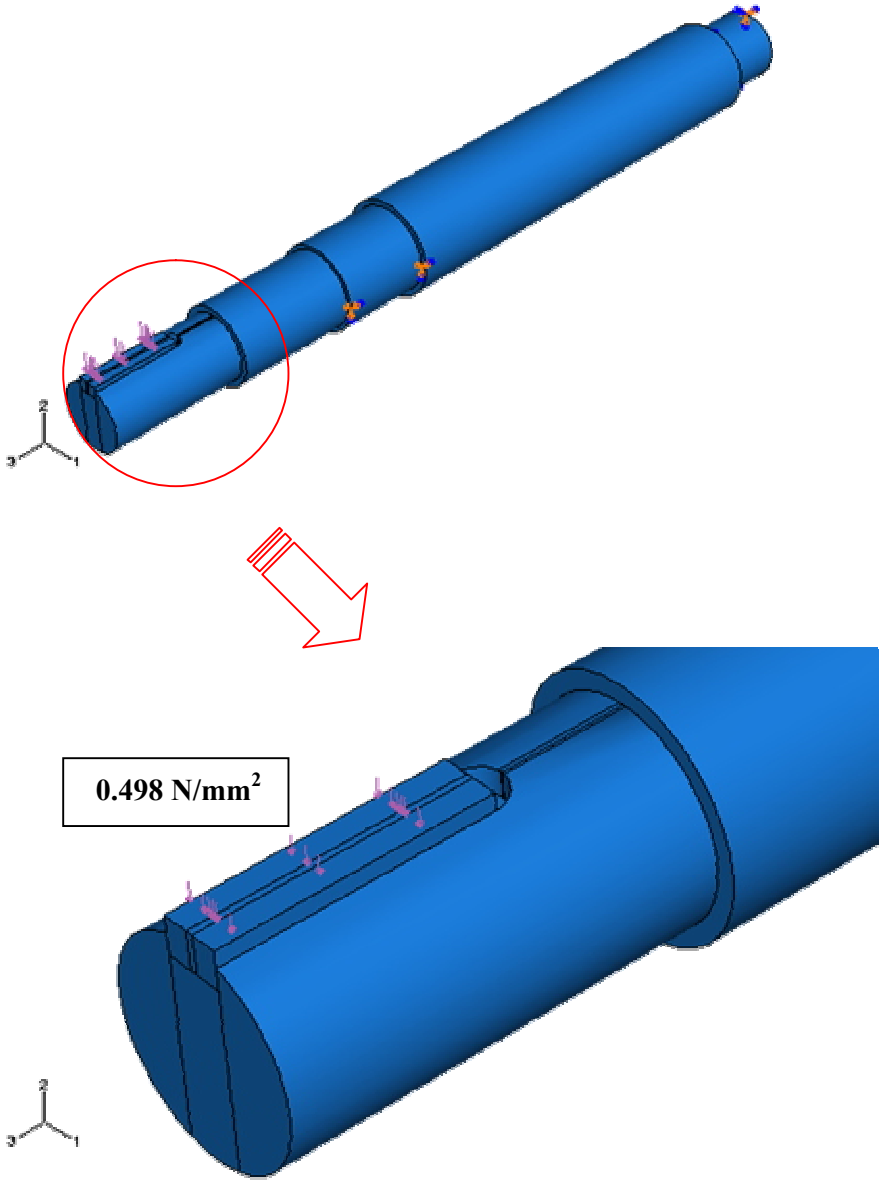

Figure 6.3: Lateral loads applied on the shaft

B. Tangential Loading

The following are the technical data specified by the manufacturer of the pump;

Power of pump, P = 30 KW

RPM, N = 1455

Therefore;

Torque, T = (60 x Power)/ (2 x 3.142 x N)

= (60 x 30000000) / (2 x 3.142 x1455)

= **196.89 KN/mm**

Tangential load = T / r

= 196.89 / 24.5

= **8,036.44 N**

So, the pressure due to the torsional loading;

Pressure = F / A

= 8,036.44 / (63 x 4.5)

= **28.35 N/mm^2**

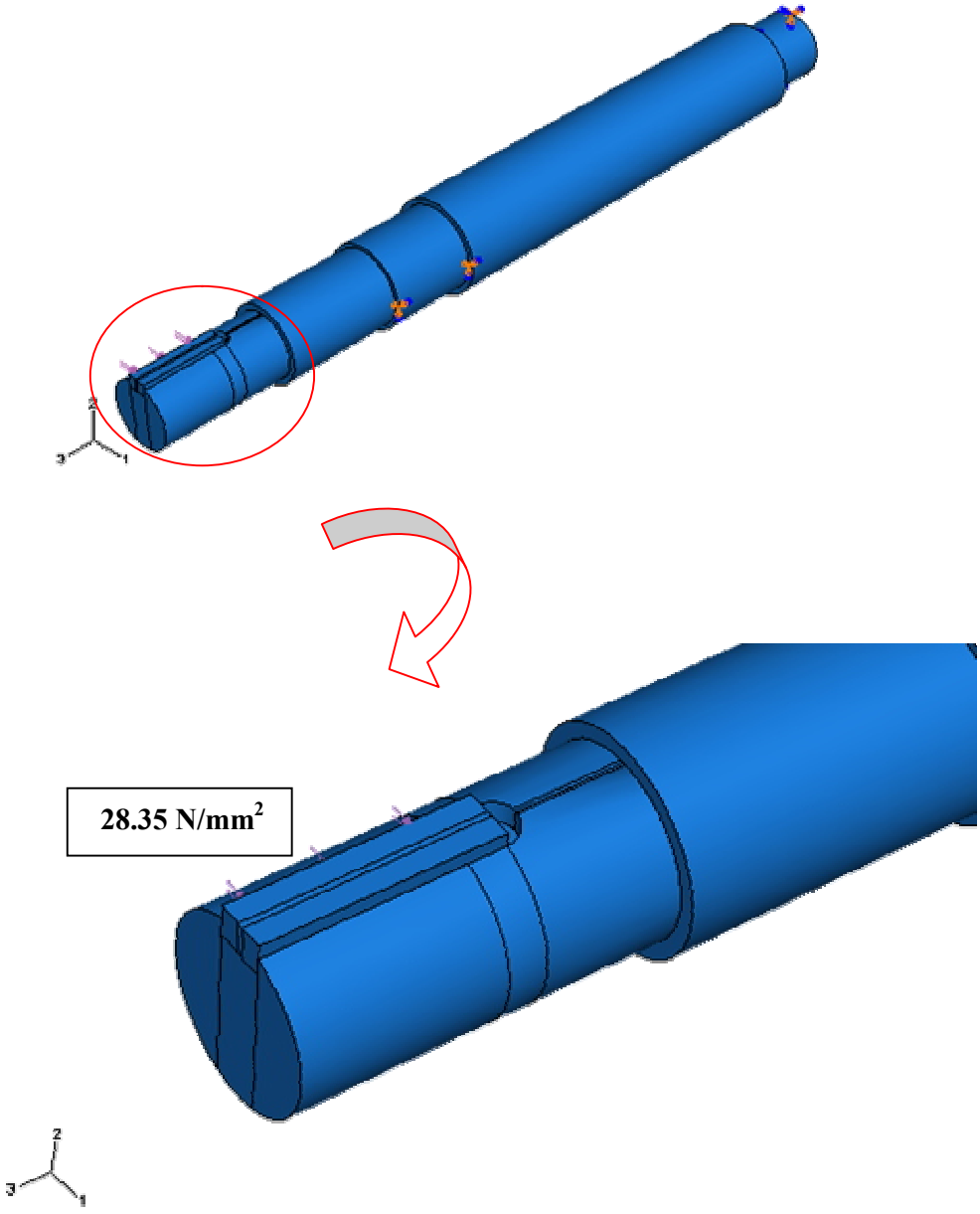

Figure 6.4: Tangential load applied on the shaft

C. Combined Loading (Lateral + Tangential)

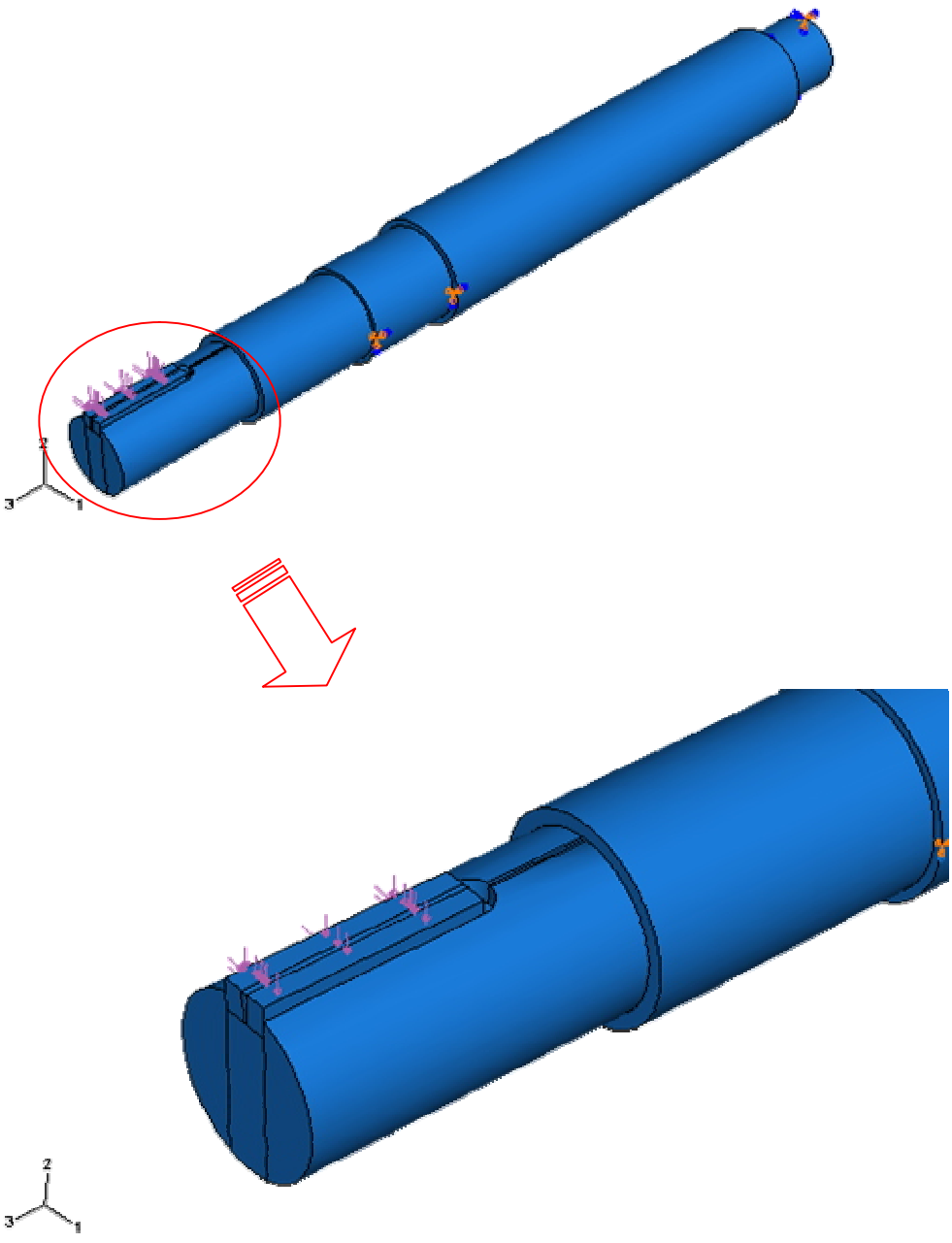

Figure 6.5: Combined Loading applied on the shaft

6.1.3 Finite Element Meshing of Shaft Model

The shaft was discretized using 2 types of finite elements, 8 node-hexagon elements for most parts of the shaft and 4 node- tetrahedral elements for the keyway area of the shaft. The details of the finite element meshing of the shaft model are as per the following;

- Total no. of Elements : 48,375

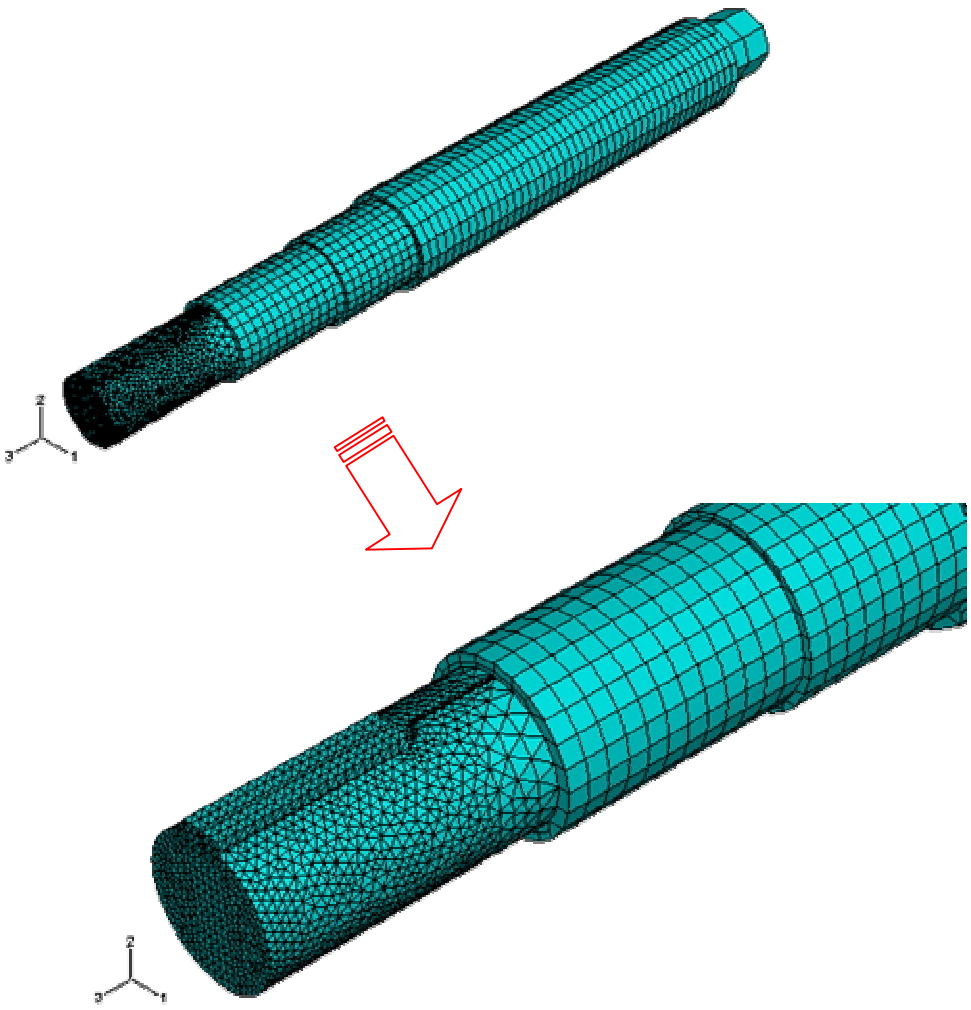

Figure 6.6: Finite Element Meshing of shaft

6.2 FATIGUE LIFE ANALYSIS

6.2.1 Modeling of shaft

The input models for the Fe-safe is imported from the same .cae and .odb file generated previously in ABAQUS. Therefore, the boundary conditions remain unchanged from the previous setting or position.

6.2.2 Loadings on Shaft

During operation, the shaft rotates while the loadings are static or the same at the same directions. Therefore, to model the input file to Fe -safe, the loadings are represented in way that the shaft is now in static position whil e the loadings fluctuate over period of time.

Basically, variation of load at any point in the shaft depends on the angular position of the shaft as it rotates. In FE -Safe, the shaft is analyzed as a stationary component. Thus, equivalent load variation per rotation of shaft is obtained through variable loading as illustrated in the figure below;

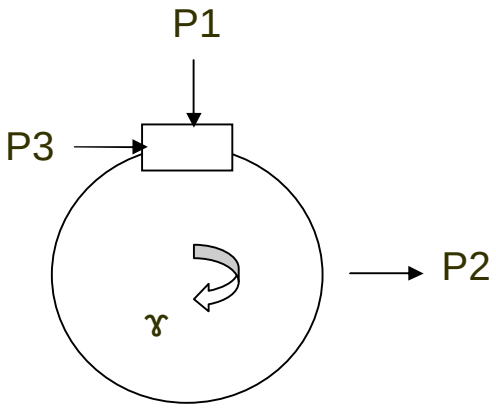

Figure 6.7: Input loadings on shaft for FE Safe

Where,

P1 & P2 represents the lateral loading and P3 represents the tangential load.

While the input files for the lateral loadings are defined as following;

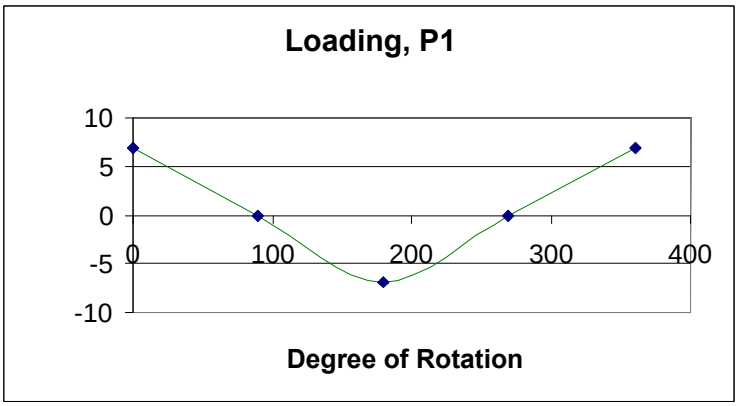

Chart 6.1: Input loading, P1, for fe-safe

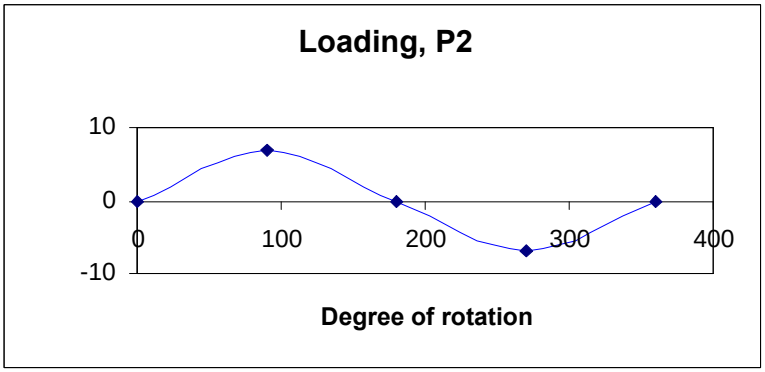

Chart 6.2: Input loading, P1, for fe-safe

CHAPTER 7

RESULTS AND DISCUSSION

7.1 FINITE ELEMENT ANALYSIS

7.1.1 Lateral Load

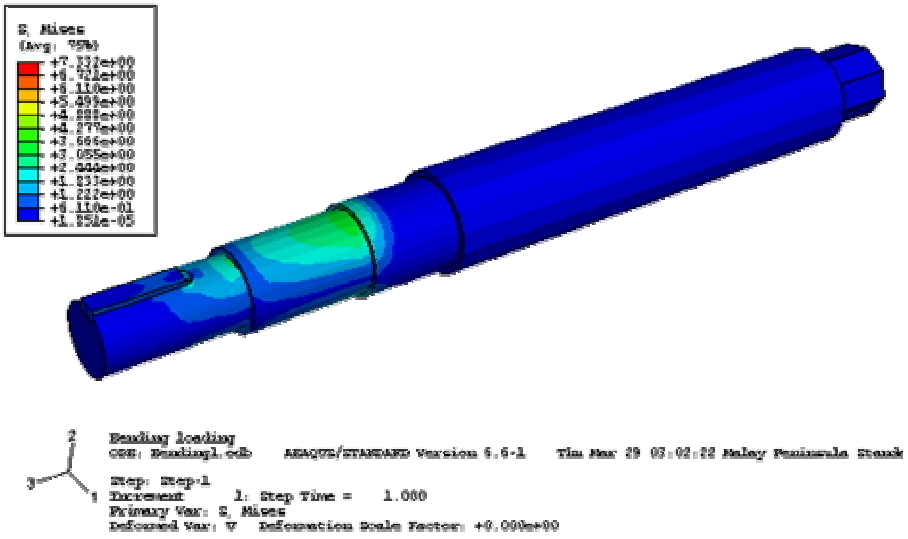

Figure 7.1: Distribution of Mises stress on shaft due to Lateral load

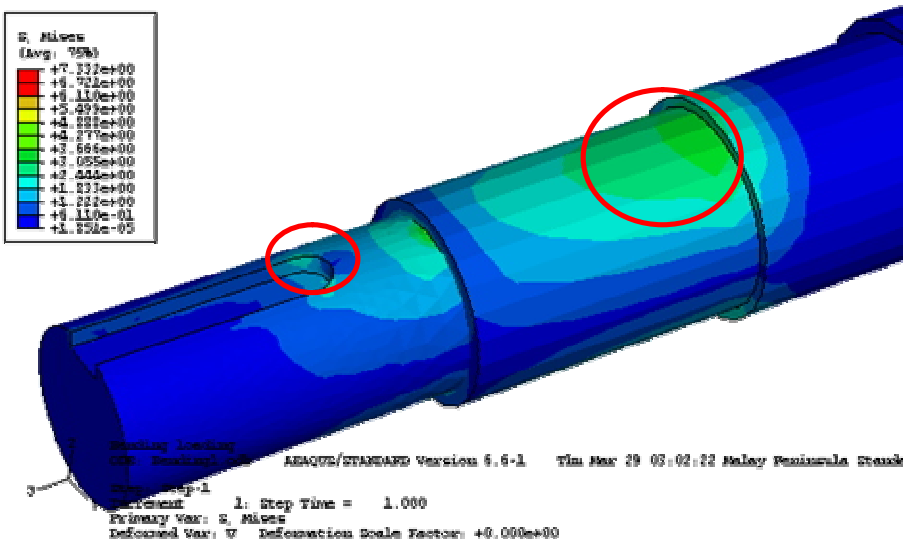

Figure 7.2: High stress concentration area due to lateral load

From the results that has been obtained, it can be seen that the higher stress concentration area are the edge of the keyway and the step down after the lower bearingós support. The Von Mises stress at the stated area is between 3 ï 4 MPa. Highest Von Mises stress is at an element located at the step down after the lower bearing support, which is about 7.332 MPa.

7.1.2 Tangential Load

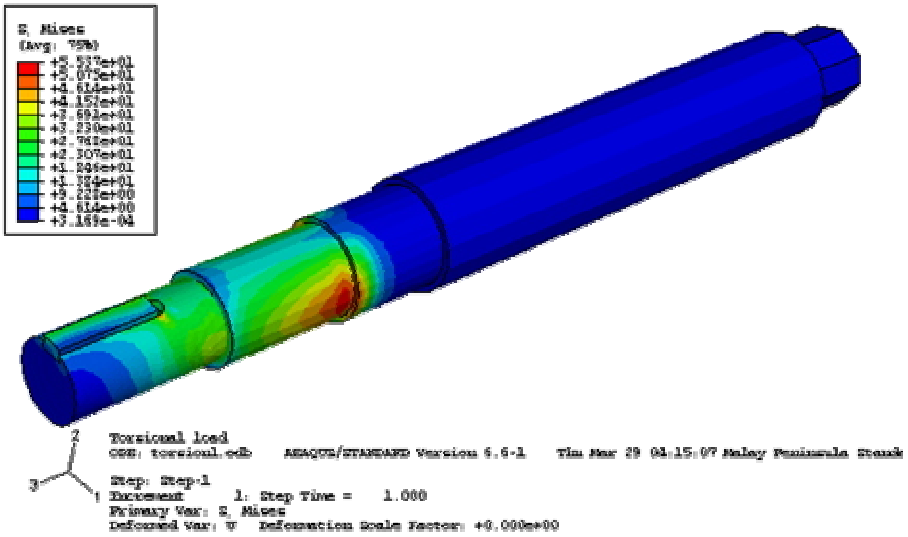

Figure 7.3: Distribution of Mises stress on shaft due to tangential load

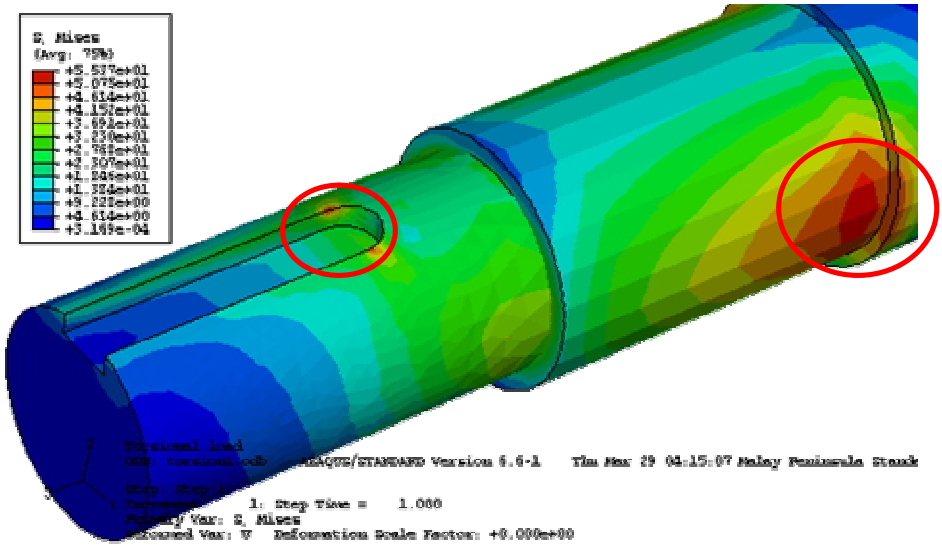

Figure 7.4: High stress concentration area due to tangential load

From the results that has been obtained, it can be seen that the higher stress concentration area are the edge of the keyway and the step down after the lower bearingós support. The Von Mises stress at the stated area is between 55.37 MPa.

7.1.3 Combined Loading (Lateral & Tangential)

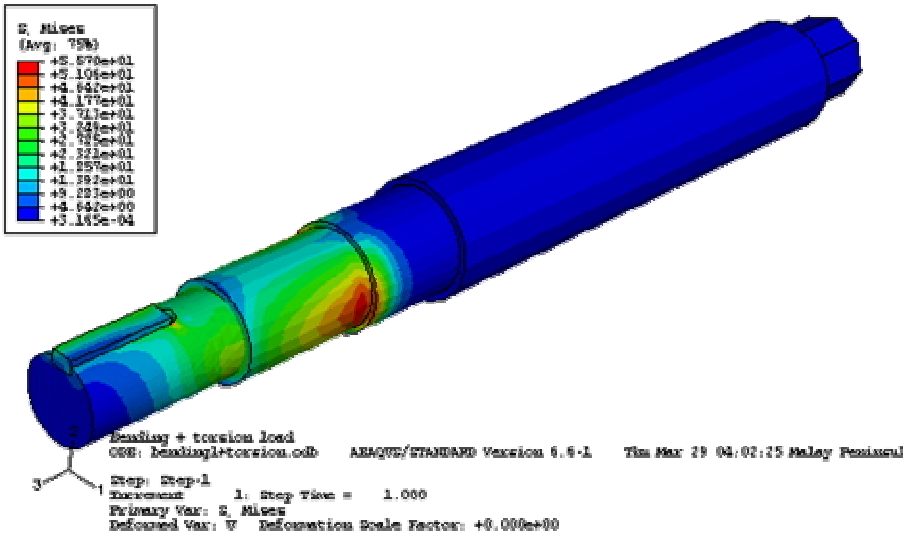

Figure 7.5: Distribution of Mises stress on shaft due to combined load

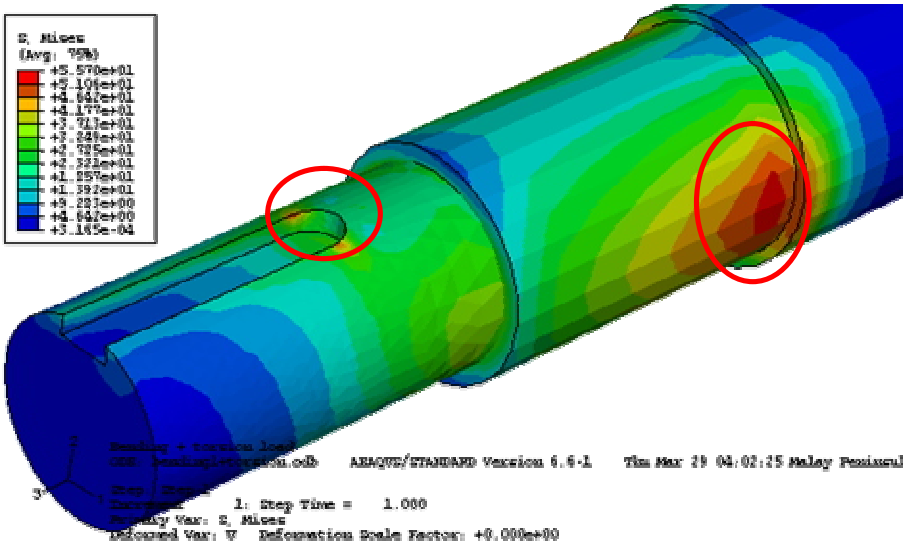

Figure 7.6: High stress concentration area due to combined load

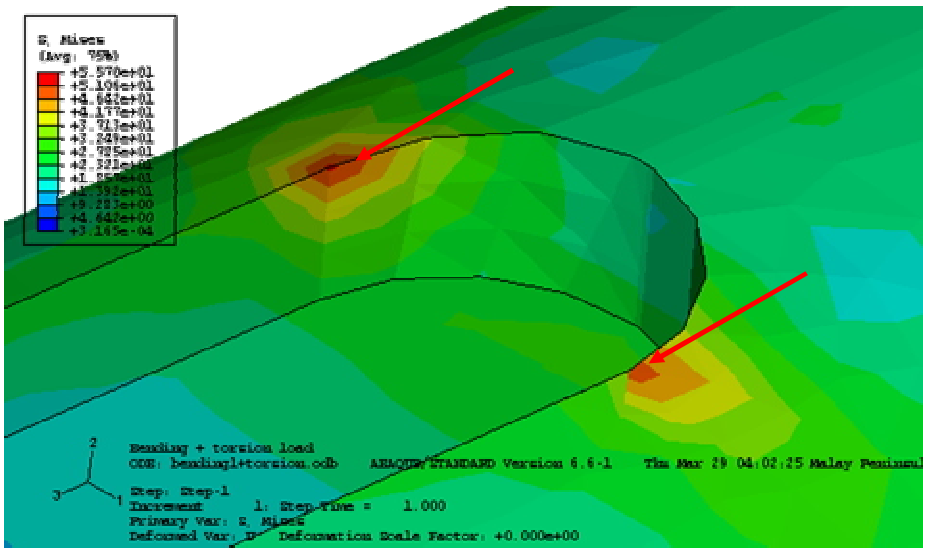

Figure 7.7: Localized high stress concentration at edge of keyway

From the results that had been obtained, it can be seen that the higher stress concentration area are still the same location but the value of von Mises stress has increased. It shows that the high stress region are very localized and the Von Mises stress at the stated area is 55.70 MPa.

7.2 FATIGUE LIFE ANALYSIS

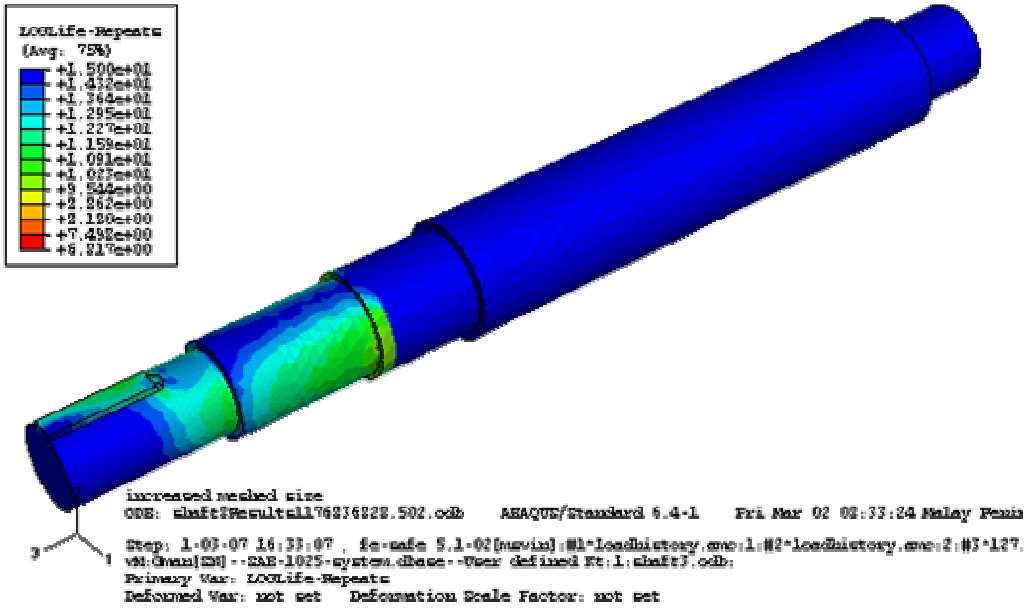

Figure 7.8: Distribution of fatigue life cycles of the shaft

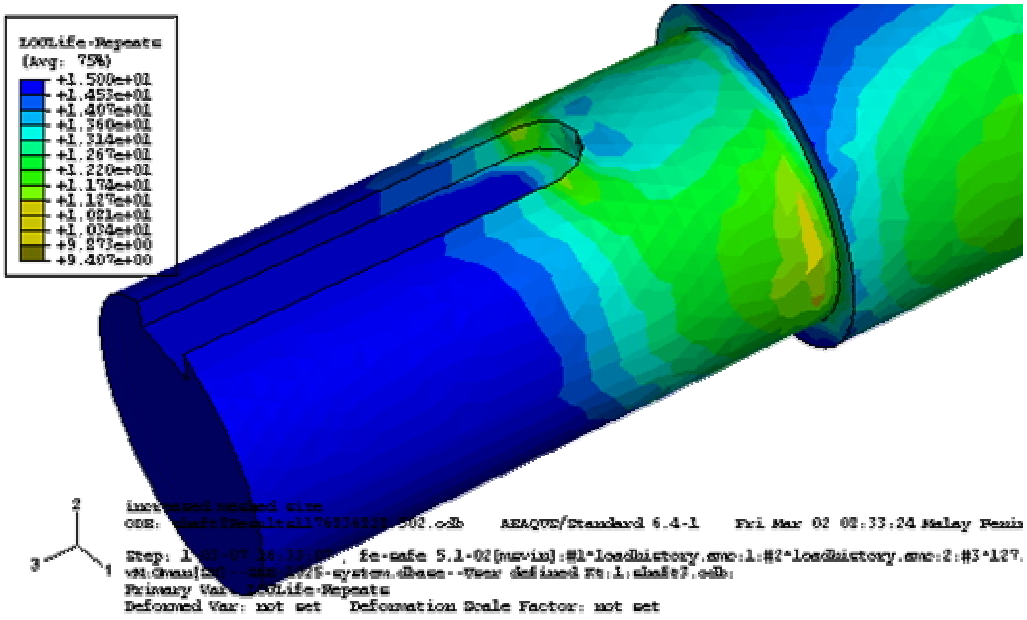

Figure 7.9: Distribution of fatigue life cycles at the critical area of the shaft

Based on the fatigue life cycle analysis that has been carried out, it can be seen that the critical life cycle of the pump shaft is between 10^6 - 10^{12} cycles. The edge of keyway, which is the critical area on the shaft has a fatigue life cycle of 10^{10} cycles.

7.3 VISUAL INSPECTION

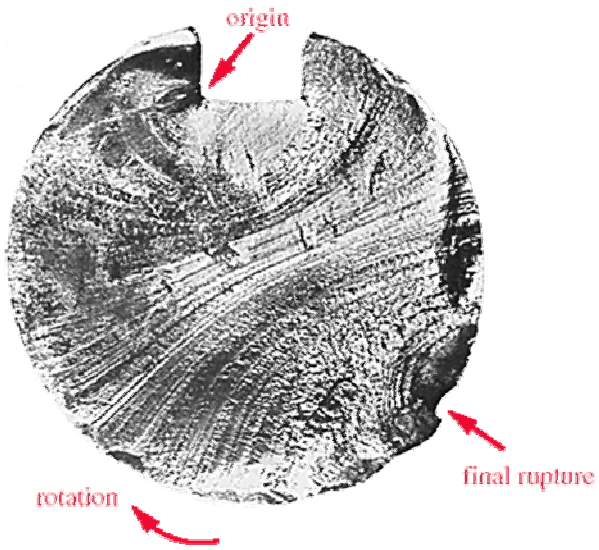

Figure 7.10: Typical contour on shaft due to bending fatigue failure

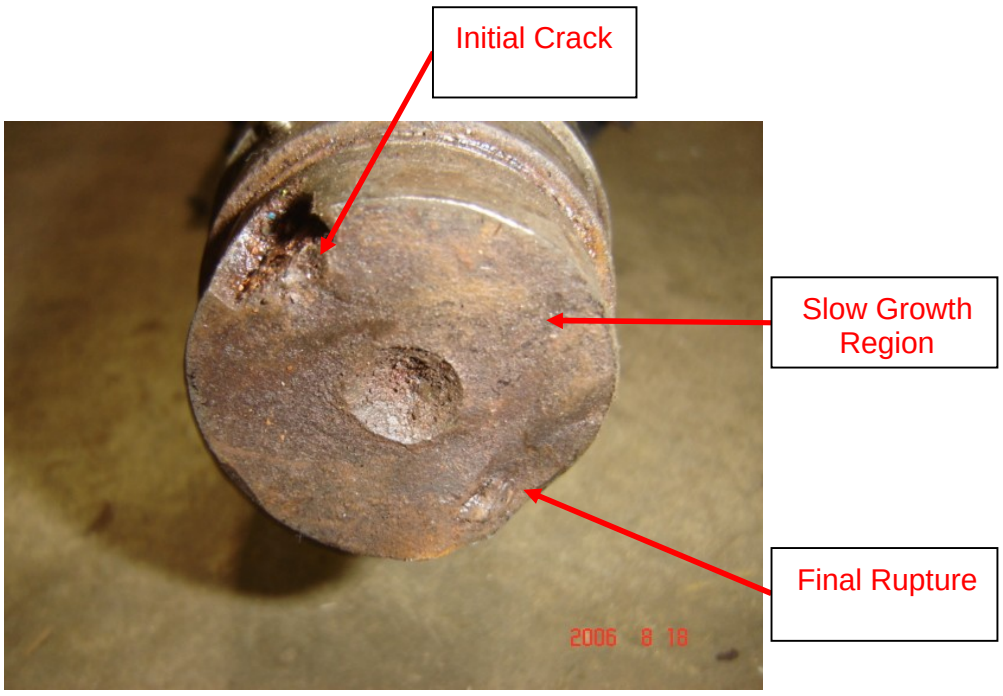

Figure 7.11: Actual contour on the failed shaft

Figure 7.12: Actual failure on the shaft

Figure 7.13: Shaft broken at high concentration area; edge of key

Based on the visual inspection or analysis on the actual failed pump shaft, it can be seen that the failure contour is similar to a bending fatigue failure contour with initial crack, slow growth region and final rupture of the shaft. The shaft actually fails at the high stress concentration region; where the edge of the key is seated on the keyway of the shaft.

One of the reasons to the failure to the shaft could be due to the oper ational condition of the shaft as well. The following picture shows the area of the shaft which is always submerged in the pumping media, which is in this case, sewage. The key is found to be always submerged in this contaminated water, where it is prune to corrode over period of time. These corrosions could lead to stress corrosion cracking which could eventually lead to fatigue failure of the shaft.

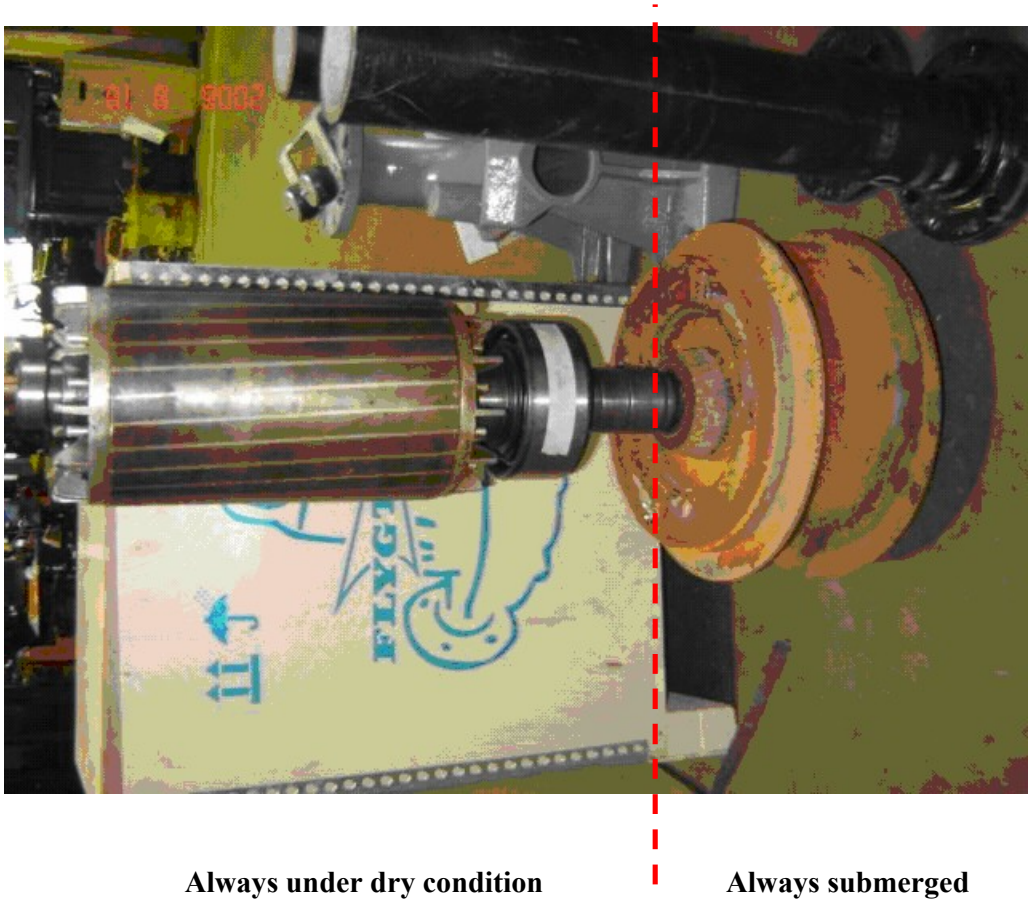

Figure 7.14: Operational position of the shaft is horizontal

CHAPTER 8

CONCLUSION

Based on the finite element analysis that has been carried out, it can be concluded that the material of the shaft has not yielded as the Von Mises stress obtained is only 55.70 MPa, which is very much less than the yield stress of the material which is 290 MPa. But the FEA analysis has given us an indication that the stress concentration at the edge of the keyway is very high compared to the other areas on the shaft.

After conducting the fatigue life cycle analysis on the shaft, we can acknowledge that the fatigue life cycle of the critical area on shaft is between 10^{6} to 10^{12} cycles and the life cycle at the edge of the keyway is about 10^{12} cycles. This shows that the shaft has been designed not to fail due to fatigue.

But the results from the visual inspection of the failed shaft are actually showing similar surface contour with a typical contour of fatigue failure. This could be due to stress corrosion factor. The shaft keyway is always submerged in water, which in this application is sewage water (dirty, contaminated, etc). Therefore, there is a high possibility of corrosion to incur in which eventually causes stress corrosion initial cracks at high stress concentration area such as the edge of key on the keyway.

Other causes to the failure of the shaft could be pitting due to corrosion and cavitations during operation of the pump. This is because pitting could cause stress raisers on the shaft which eventually leads to fatigue failure. Besides that, a defect on the surface of the shaft during manufacturing processes could also lead to initial cracks to occur when the shaft is in operation. This imperfection on the surface finish creates high stress concentration zone where the cracks develops during operation of the shaft over period of time.

Since the shaft has been designed for infinite life, these other factors are suspected to be the main contributors to the failure of the shaft, mainly due to fatigue under cyclic loading when it is in operation.

REFERENCES

1. Joseph E. Shigley Charles R. Mischke. *Mechanical Engineering Design*, 5th Edition: McGraw Hill International Edition; 1989.
2. Austin H.Bounett. The cause and Analysis of Bearing and Shaft Failures: *EASA Technical Note*; 1999.
3. ITT Industries (Flygt). Shaft and Bearing Calculations; 2004.
4. ITT Industries (Flygt). Materials; 2000.
5. Dr. Andrei Lozzi. Shafts and Axles: *School of Aerospace, Mechanical and Mechatronic Engineering*; 2006.
6. Noah N. Mauring. Designing the shaft diameter for acceptable level of stress: *Journal of Mechanical Design*; 2000.
7. R.E Peterson. Stress Concentration Factors; 1974.
8. G.L Huyett. Engineering Handbook; 2004.
9. Stuart H. Loewenthal. Design of power transmitting shaft: *NASA Publications 1123*; 1984.
10. Bruno Conegliano. Sewers ï Lifting Station: *Environmental Publisher Association*; 2000.
11. ITT Industries (Flygt): *Technical Specifications C3201*; 2000.
12. Arthur Marczewski. Numerical Fatigue Analysis of cracked rotor; 2004.
13. K. Holmedahl. Prediction of High Cycle Fatigue; 1999.
14. Dr. Robert Adey. Fatigue Life & crack growth prediction; 2004.
15. Dr. Joe Evans. Sewage pump impeller selection; 2000.
16. Dr. Jean C. Bailey. Forces on centrifugal pump impeller; 1985.
17. SEW Eurodrive. Torque Advantages: *Technical note*; 2006.
18. McNally. Shaft Deflection & Bending Formula; 2000.
19. Fe-safe Brochure 1/rev5: *Safe Technology ltd;* 1999.

20. Fe-safe user manual: *Safe Technology ltd*; 2003.

21. Abaqus user manual: *ABAQUS Inc*; 2001.

APPENDIX A

PRELIMINARY FATIGUE LIFE ANALYSIS

1. Location F

D = 72.10 mm
d = 63.45 mm
r = 3 mm

D/d = 72.10 / 63.45 = 1.14
r/d = 3/ 63.45 = 0.05

- Based on Figure A-15-9 (Shigley/Mischke: Mech. Eng. Design, 5th Edition), the value of theoretical stress concentration factor, is given as $K_t = 2.05$.

- Based on Figure 5-16 (Shigley/Mischke: Mech. Eng. Design, 5th Edition), the value of notch sensitivity, is given as q = 0.78.

Therefore, fatigue stress concentration factor;

$K_f = 1 + q(Kt ï 1)$
$= 1 + 0.78(2.05 -1)$
$= 1.819$

fatigue strength reduction factor, K_e becomes;

$K_e = 1/ k_f$

$= 1/ 1.819$

$= \underline{0.55}$

Now, Endurance limit becomes;

$S_e = K_aK_bK_cK_dK_eS_e\hat{o}$

$= 0.874 \times 0.75 \times 1 \times 1 \times 0.55 \times 246.96$

$= \mathbf{\underline{89.04\ MPa}}$

Calculating bending stress at location F;

Bending moment at location F = <u>132.03 Nm</u>

Bending stress, $\boldsymbol{\sigma_a} = \mathbf{32M/ \pi d^3}$

$= (32 \times 132.03) / (3.142 \times 0.06345^3)$

$= \mathbf{\underline{5.27\ MPa}}$

This stress is lower than the endurance limit, and so, the part will have infinite life.

Calculating estimated life of part;

$$\mathbf{N = (\sigma_a/a)^{1/b}}$$

Where,

$\mathbf{a = (0.9 \times S_t^2) / S_e}$ &

$\mathbf{b = -1/3 \times \log (0.9 \times S_t) / S_e}$

$a = (0.9 \times 490^2) / 89.04 = \underline{2426.89}$

$b = -1/3 \times \log (0.9 \times 490) / 89.04 = -0.2316$

Estimated life of part, $N = (\mathring{u}_a/a)^{1/b}$

$= (5.27/2426.89)^{-1/0.2316}$

$= \mathbf{3.16 \times 10^{11} \text{ cycles.}}$

Bending moment at location F = 132.03 Nm

Bending stress, $\boldsymbol{\sigma_a}$ $= \mathbf{32M/ \pi d^3}$

$= (32 \times 132.03) / (3.142 \times 0.06345^3)$

$= \mathbf{5.27 \text{ MPa}}$

Shear stress, $\not{\epsilon}_{xy}$ $= \mathbf{16T/ \pi d^3}$

$= (16 \times 200) / (3.142 \times 0.06345^3)$

$= \mathbf{3.99 \text{ MPa}}$

therefore, the two non zero principle stresses from Mohr circle analysis becomes;

$\boldsymbol{\sigma_A, \sigma_B} = \mathbf{(\sigma_a/2) \pm [(\sigma_a/2)^2 + T_{xy}^2]^{1/2}}$

$= (5.27/2) \tilde{N}[(5.27/2)^2 + 3.99^2]^{1/2}$

$= (2.635) \tilde{N}[(6.943) + 15.92]^{1/2}$

$= 2.635 \tilde{N}[4.782]$

$\mathring{u}_A = 2.635 + [4.782] =$ 7.417 MPa

$\mathring{u}_B = 2.635 - [4.782] =$ -2.147 MPa

Calculating Von Mises Stress, $\mathring{u}^{\hat{o}}$:

$\boldsymbol{\sigma' = (\sigma_A^2 - \sigma_A \sigma_B + \sigma_B^2)^{1/2}}$

$= (7.417^2 \text{ ï } (7.417 \times -2.147) + (-2.147)^2)^{1/2}$

$= \mathbf{8.69 \text{ MPa}}$

Lastly, estimated factor of safe guarding against fatigue failure ;

$n = Se / \mathring{u}^{\hat{o}}$

$= 89.04 / 8.69$

$= \mathbf{10.25}$

2. Location G

D = 63.45 mm

d = 57.68 mm

r = 3 mm

D/d = 63.45 / 57.68 = 1.10

r/d = 3/ 57.68 = 0.05

- Based on Figure A-15-9 (Shigley/Mischke: Mech. Eng. Design, 5th Edition), the value of theoretical stress concentration factor, is given as K_t = 1.95.

- Based on Figure 5-16 (Shigley/Mischke: Mech. Eng. Design, 5th Edition), the value of notch sensitivity, is given as q = 0.78.

Therefore, fatigue stress concentration factor;

K_f = 1 + q(Kt ï 1)

= 1 + 0.78(1.95 -1)

= 1.741

Fatigue strength reduction factor, K_e becomes;

K_e = 1/ k_f

= 1/ 1.741

= 0.574

Now, Endurance limit becomes;

S_e = $K_aK_bK_cK_dK_eS_e$ô

= 0.874 x 0.75 x 1 x 1 x 0.574 x 246.96

= **92.92 MPa**

Calculating bending stress at location G;

Bending moment at location G = 111.09 Nm

Bending stress, σ_a $= 32M/ \pi d^3$

$= (32 \times 111.09) / (3.142 \times 0.05768^3)$

$=$ **5.90 MPa**

This stress is lower than the endurance limit, and so, the part will have infinite life.

Calculating estimated life of part;

$$N = (\sigma_a/a)^{1/b}$$

Where,

$a = (0.9 \times S_t^2) / S_e$ &

$b = -1/3 \times \log (0.9 \times S_t) / S_e$

$a = (0.9 \times 490^2) / 92.92 =$ 2325.55

$b = -1/3 \times \log (0.9 \times 490) / 92.92 =$ -0.2254

Estimated life of part, $N = (\mathring{u}_a/a)^{1/b}$

$= (5.90/2325.55)^{-1/0.2254}$

$=$ **3.28×10^{11} cycles.**

Bending moment at location G = 111.09 Nm

Bending stress, σ_a $= 32M/ \pi d^3$

$= (32 \times 111.09) / (3.142 \times 0.05768^3)$

$=$ **5.90 MPa**

Shear stress, ϕ_{xy} $= 16T/ \pi d^3$

$= (16 \times 200) / (3.142 \times 0.05768^3)$

$=$ **5.31 MPa**

Therefore, the two non zero principle stresses from Mohr circle analysis becomes;

$$\sigma_A, \sigma_B = (\sigma_a/2) \pm [(\sigma_a/2)^2 + T_{xy}^2]^{1/2}$$

$$= (5.90/2) \tilde{N}[(5.90/2)^2 + 5.31^2]^{1/2}$$

$$= (2.95) \tilde{N}[(8.7025) + 28.196]^{1/2}$$

$$= 2.95 \tilde{N}[6.07]$$

$\mathring{u}_A = 2.95 + [6.07] =$ <u>9.02 MPa</u>

$\mathring{u}_B = 2.95 - [6.07] =$ <u>-3.12 MPa</u>

Calculating Von Mises Stress, $\mathring{u}^{\hat{o}}$:

$$\sigma' = (\sigma_A^2 - \sigma_A \sigma_B + \sigma_B^2)^{1/2}$$

$$= (9.02^2 \ddot{i} (9.02 \times -3.12) + (-3.12)^2)^{1/2}$$

$$= \underline{\mathbf{10.92\ MPa}}$$

Lastly, estimated factor of safe guarding against fatigue failure ;

$$n = Se / \mathring{u}^{\hat{o}}$$

$$= 92.92 / 10.92$$

$$= \underline{\mathbf{8.51}}$$

3. Location H

D = 57.68 mm

d = 49.03 mm

r = 3 mm

D/d = 57.68 / 49.03 = 1.18

r/d = 3/ 49.03 = 0.06

- Based on Figure A-15-9 (Shigley/Mischke: Mech. Eng. Design, 5th Edition), the value of theoretical stress concentration factor, is given as $K_t = 1.95$.

- Based on Figure 5-16 (Shigley/Mischke: Mech. Eng. Design, 5th Edition), the value of notch sensitivity, is given as q = 0.78.

Therefore, fatigue stress concentration factor;

K_f = 1 + q(Kt ï 1)

= 1 + 0.78(1.95 -1)

= 1.741

Fatigue strength reduction factor, K_e becomes;

K_e = 1/ k_f

= 1/ 1.741

= 0.574

Now, Endurance limit becomes;

S_e = $K_aK_bK_cK_dK_eS_e$ô

= 0.874 x 0.75 x 1 x 1 x 0.574 x 246.96

= **92.92 MPa**

Calculating bending stress at location H;

Bending moment at location H = 58.99 Nm

Bending stress, σ_a $= 32M/ \pi d^3$

$= (32 \times 58.99) / (3.142 \times 0.04903^3)$

$= \mathbf{5.10\ MPa}$

This stress is lower than the endurance limit, and so, the part will have infinite life.

Calculating estimated life of part;

$$N = (\sigma_a/a)^{1/b}$$

Where,

$a = (0.9 \times S_t^2) / S_e$ &

$b = -1/3 \times \log (0.9 \times S_t) / S_e$

$a = (0.9 \times 490^2) / 92.92 = 2325.55$

$b = -1/3 \times \log (0.9 \times 490) / 92.92 = -0.2254$

Estimated life of part, $N = (\mathring{u}_a/a)^{1/b}$

$= (5.10/2325.55)^{-1/0.2254}$

$= \mathbf{6.26 \times 10^{11}\ cycles.}$

Bending moment at location H = 58.99 Nm

Bending stress, σ_a $= 32M/ \pi d^3$

$= (32 \times 58.99) / (3.142 \times 0.04903^3)$

$= \mathbf{5.10\ MPa}$

Shear stress, ϕ_{xy} $= 16T/ \pi d^3$

$= (16 \times 200) / (3.142 \times 0.04903^3)$

$= \mathbf{8.64\ MPa}$

Therefore, the two non-zero principle stresses from Mohr circle analysis becomes;

$\sigma_A, \sigma_B = (\sigma_a/2) \pm [(\sigma_a/2)^2 + T_{xy}^2]^{1/2}$

$= (5.10/2)$ Ñ$[(5.10/2)^2 + 8.64^2]^{1/2}$

$= (2.55)$ Ñ$[(6.5025) + 74.65]^{1/2}$

$= 2.55$ Ñ$[9.01]$

$\mathring{u}_A = 2.55 + [\ 9.01] =$ 11.56 MPa

$\mathring{u}_B = 2.55 - [\ 9.01] =$ -6.46 MPa

Calculating Von Mises Stress, $\mathring{u}^{\hat{0}}$:

$\sigma' = (\sigma_A^2 - \sigma_A \sigma_B + \sigma_B^2)^{1/2}$

$= (11.56^2$ ï $(11.56 \times -6.46) + (-6.46)^2)^{1/2}$

$= \mathbf{15.81MPa}$

Lastly, estimated factor of safe guarding against fatigue failure ;

$n = Se / \mathring{u}^{\hat{0}}$

$= 92.92 / 15.81$

$= \mathbf{5.88}$

4. Location I (Keyway)

D = 57.68 mm

d = 49.03 mm

r = 3 mm

D/d = 57.68 / 49.03 = 1.18

r/d = 3/ 49.03 = 0.06

- Based on R.E Peterson, Stress concentration factors, the value of theoretical stress concentration factor for keyway, is given as $K_t = 1.79$.

- Based on Figure 5-16 (Shigley/Mischke: Mech. Eng. Design, 5th Edition), the value of notch sensitivity, is given as q = 0.78.

Therefore, fatigue stress concentration factor;

$K_f = 1 + q(Kt - 1)$

$= 1 + 0.78(1.79 - 1)$

$= 1.6162$

fatigue strength reduction factor, K_e becomes;

$K_e = 1/ k_f$

$= 1/ 1.6162$

$= 0.619$

Now, Endurance limit becomes;

$S_e = K_aK_bK_cK_dK_eS_e\hat{o}$

$= 0.874 \times 0.75 \times 1 \times 1 \times 0..619 \times 246.96$

$=$ **100.21 MPa**

Calculating bending stress at location I;

Bending moment at location I = 41.92 Nm

Bending stress, σ_a $= 32M/ \pi d^3$

$= (32 \times 41.92) / (3.142 \times 0.04903^3)$

$=$ **3.62 MPa**

This stress is lower than the endurance limit, and so, the part will have infinite life.

Calculating estimated life of part;

$$N = (\sigma_a/a)^{1/b}$$

Where,

$a = (0.9 \times S_t^2) / S_e$ &

$b = -1/3 \times \log (0.9 \times S_t) / S_e$

$a = (0.9 \times 490^2) / 100.21 =$ 2156.37

$b = -1/3 \times \log (0.9 \times 490) / 100.21 =$ -0.2145

Estimated life of part, $N = (\mathring{u}_a/a)^{1/b}$

$= (3.62/2156.37)^{-1/0.2145}$

$=$ **8.65×10^{12} cycles.**

Bending moment at location I = 41.92 Nm

Bending stress, σ_a $= 32M/ \pi d^3$

$= (32 \times 41.92) / (3.142 \times 0.04903^3)$

$= \mathbf{3.62\ MPa}$

Shear stress, ϕ_{xy} $= 16T/ \pi d^3$

$= (16 \times 200) / (3.142 \times 0.04903^3)$

$= \mathbf{8.64\ MPa}$

therefore, the two non zero principle stresses from Mohr circle analysis becomes;

$\sigma_A, \sigma_B = (\sigma_a/2) \pm [(\sigma_a/2)^2 + T_{xy}^2]^{1/2}$

$= (3.62/2)$ Ñ$[(3.62/2)^2 + 8.64^2]^{1/2}$

$= (1.81)$ Ñ$[(3.276) + 74.65]^{1/2}$

$= 1.81$ Ñ$[8.83]$

$\mathring{u}_A = 1.81 + [\ 8.83] =$ 10.64 MPa

$\mathring{u}_B = 1.81 - [\ 8.83] =$ -7.02 MPa

Calculating Von Mises Stress, $\mathring{u}^{\hat{0}}$:

$\sigma' = (\sigma_A^2 - \sigma_A \sigma_B + \sigma_B^2)^{1/2}$

$= (10.64^2$ ï $(10.64 \times -7.02) + (-7.02)^2)^{1/2}$

$= \mathbf{15.40MPa}$

Lastly, estimated factor of safe guarding against fatigue failure ;

$n = Se / \mathring{u}^{\hat{0}}$

$= 124.81/ 15.40$

$= \mathbf{8.11}$